

Characterization of NaChBac in Artificial Lipid Bilayer Membrane

By

Andrew Jo

A thesis submitted in partial fulfillment of the requirements for the degree of

Master of Science

in

Chemical Engineering

Department of Chemical and Materials Engineering

University of Alberta

© Andrew Jo, 2016

Abstract

NaChBac is a voltage-gated Na^+ channel from the bacterium *Bacillus haloduran*. Studying this protein channel can help researchers discover potential pharmaceuticals, innovative strategies in eliminating biofilms, and could be used to improve desalinization technologies. This thesis will discuss the characterization of NaChBac in artificial lipid membrane, including single molecule study on the conductance and ion selectivity using a planar bilayer membrane device and the development of a scattered light based stopped-flow flux assay.

Planar lipid bilayer membrane is a common technique to characterize ion channel function. In this thesis, purified NaChBac protein was incorporated into lipid vesicles which were then fused to a planar lipid bilayer. By applying a controllable electrical potential (i.e. voltage) across the protein-embedded bilayer and measuring the resulting current, the conductance, gating behaviour, and ion selectivity of the open channel were studied. NaChBac was found to have three conductance levels at 268.5 ± 45.2 pS (mean \pm SEM, $n=2$), 92.8 ± 18.0 pS ($n=3$), and 26.4 ± 5.6 pS ($n=4$), respectively. Its activation gating voltage ($V_{1/2}$) is -28 mV and its apparent activation gating charge is 15.9 elementary charge. NaChBac tested under asymmetric saline buffer solution conditions was shown to have a relative permeability $P_{\text{Na}^+}/P_{\text{K}^+}$ ranging from 0.86 to 1.35 and $P_{\text{Na}^+}/P_{\text{Ca}^{2+}} = 1.43 \pm 0.20$ ($n=3$, \pm SEM).

Conventional flux assay for ion channels requires the use of ion-specific dyes. However, the availability of the dyes and their selectivity limits the spectrum of ion channels that can be tested in a fluorescence flux assay. Instead, stopped-flow spectrometry can be used to monitor the change in size of the protein-incorporating

vesicles that is caused by ion flux, which is in turn triggered by the transmembrane electrochemical gradient of the target ion species. With this method, the ion conducting function of purified NaChBac protein was shown. The method can potentially be used to test the functionality of other ion channels.

Preface

This thesis is an original work by Andrew Jo supervised by Dr. Carlo Montemagno. No part of this thesis has been previously published.

Acknowledgement

I would like to acknowledge Dr. Carlo Montemagno as my supervisor and Dr. Hiofan Hoi as my mentor for their feedback and suggestions. I would like to thank Drs. Hyo-Jick Choi, Manisha Gupta and Klaus Ballanyi for their time spent reviewing my thesis and attending my thesis defense. I would like to thank Hang Zhou for technical assistance on the purification, Jack Moore for the MS analysis, and Ed Buck for training on the Warner Bilayer system. I would also like to thank Mark Rozema and Ankit Kumar for supporting me through my Masters program.

Contents

Chapter 1	Introduction.....	1
1.1	Hodgkin and Huxley's model on electrical current passing cell membrane	4
1.2	Voltage-gated ion channel and NaChBac	6
1.3	BLM technique	7
1.3.1	BLM device for membrane protein studies	7
1.3.2	Advantages and disadvantages of BLM	12
1.4	Scope of work and challenges.....	14
Chapter 2	Summary on Materials and Methods.....	16
2.1	Materials and instruments	17
2.2	Methods	19
2.2.1	Recombinant overexpression and purification of NaChBac.....	19
2.2.2	Liposome preparation and NaChBac incorporation	21
2.2.3	Fluorescence flux assay with fluorometer.....	24
2.2.4	Perfusion of BLM chambers	25
2.2.5	Incorporation of protein onto BLM by vesicle fusion	25
2.2.6	Single channel recording using BLM	26
2.2.7	Gel filtration chromatography and polydispersity measurement of liposomes	31

2.2.8 NaChBac functionality by scattered light stopped-flow spectroscopy . 32

Chapter 3 Protein Purification and Functional Characterization of NaChBac with Fluorescence Flux Assay	33
3.1 Introduction	34
3.1.1 Incorporation of membrane proteins into liposomes	34
3.1.2 Fluorescence flux assay	37
3.2 Results and discussion.....	38
3.2.1 Recombinant overexpression and purification of NaChBac.....	38
3.2.2 Encapsulation Efficiency.....	41
3.2.3 Functional characterization of NaChBac with dye-based flux assay...	44
3.3 Conclusion	46
Chapter 4 Using Planar Bilayer Membranes to Characterize NaChBac.....	47
4.1 Introduction	48
4.1.1 Capacitive current.....	49
4.1.2 Permeability of K^+ and Ca^{2+}	53
4.2 Results and discussion.....	57
4.2.1 General set-up of the Bilayer workstation to characterize NaChBac ..	57
4.2.2 Conductance measurement of NaChBac	59
4.2.3 Activation voltage of NaChBac by single channel recording.....	77
4.2.4 Selectivity study of NaChBac with BLM	81

4.2.5 Conclusions	87
Chapter 5 Using Scattered Light Stopped-flow Spectroscopy to Study NaChBac	
89	
5.1 Introduction	90
5.1.1 Advantages of using scattered light stopped-flow spectroscopy.....	90
5.1.2 Light scattering intensity changes of liposome	91
5.2 Results and discussion.....	93
5.2.1 NaChBac vesicles functionailty by scattered light stopped-flow spectroscopy	93
5.3 Conclusion	99
Chapter 6 Conclusions and Future Directions.....	100
References	103

List of Tables

Table 2.1. Table of buffers used to hydrate liposome powder for each experiment.	24
Table 4.1. Offset voltages for different buffer conditions. Values were obtained from a single measurement.....	59

Table 4.2. Conductance and E_{rev} of 6His-NaChBac under different NaCl concentrations. One measurement was done for each condition..... 61

Table 4.3. The conductance of NaChBac in pS as obtained from single channel recording with 150 mM NaCl in both cis and trans chamber. Drug was added so there would be 4 mM of lidocaine n-ethyl bromide in the trans chamber. NA means that no current peak was found and ND means that the experiment did not take place..... 71

Table 4.4. Components and relative concentrations in the purified NaChBac sample determined by SDS-PAGE and LC-MS. 75

Table 4.5. Na^+/K^+ selectivity of NaChBac. For Trial 2 and 3, two sub-states were found (denoted as a and b respectively) thus two E_{rev} and two relative permeability values can be derived. 86

Table 4.6. Na^+/Ca^{2+} selectivity of NaChBac..... 86

Table 5.1. Size and polydispersity of liposome samples before and after Gel Filtration chromatography. The fraction highlighted in bold was used in the stopped-flow spectroscopy in the experiment discussed in Section 5.2.1..... 96

Table 5.2. Diameter of the liposome vesicles used in the stopped-flow by using DLS instrument in the experiment found in Figure 5.2. 99

List of Figures

Figure 1.1. Illustration of a BLM workstation. (a) A picture of the BLM workstation used in this thesis. As labeled, it consists of a BLM headstage (1), Ag/AgCl electrodes (2), agar salt bridges (3), a trans chamber (4), a cis chamber (5), a stirring apparatus (6), and a perfusion setup (7). The above accessories are enclosed in a Faraday cage (not shown here), which serves to reduce electrical noise. (b) A schematic representation of the bilayer workstation. The reference electrode is in the trans chamber and the command electrode is in the cis chamber. (c) A simplified current schematic which represents the bilayer workstation with a lipid membrane. V_s is the voltage source, R_m is the resistance due to the lipid membrane bilayer, C_m is the capacitance due to the lipid membrane bilayer, R_{elec} is the resistance due to the electrodes, I_{in-} is the current that is to be amplified, V_{out} is the voltage that is amplified from I_{in-} 8

Figure 1.2. Schematic of an inverting amplifier..... 10

Figure 1.3. Schematic representation of the vesicles fusion onto the BLM. 12

Figure 2.1. Using Clampfit, the peak currents to plot the I-V graph can be determined. (a) An example of a current trace recording (b) The Single Channel Search window (c) The All point histogram window..... 29

Figure 2.2. Voltage protocols used to find E_{rev} . (a) Bi-ionic protocol (b) Voltage ramp protocol. 31

Figure 3.1. The HIS-tag of NaChBac was cleaved and verified using SDS-PAGE and dot blot test. (a) Pseudo-native SDS-PAGE gel of 6His-tagged and tag-cleaved NaChBac. Lane 1: protein standards (PageRuler Easy Plus, Thermo Scientific); lane 2: 6His-tagged NaChBac incubated with thrombin for 12 h; lane 3: 6His-tagged NaChBac without thrombin treatment; lane 4: mixture of both types of NaChBac. b) The dot blot test which tests for the 6His-tag on the NaChBac cleaved protein. 2 μ l of each sample at 50 μ g/ml was applied. Spot 1 is NaChBac after thrombin digestion and spot 2 is a positive control that contains KvAP with 6His-tag. 40

Figure 3.2. Fluorescence of Sodium Green (SG) in liposome samples prepared by different encapsulation techniques. (a) Difference in fluorescence spectra of the SG-containing liposome upon salt-treatment. Samples were prepared by sonication (red), direct hydration (blue), or freeze thaw (green) and tested without (dash line) and with (solid line) the presence of Triton X-100. (b) Ratio of the intensity change of the samples after and before lysis for each encapsulation method used. 43

Figure 3.3. Schematic representation and experimental result of the fluorescence flux assay with SG. (a) The vesicle samples were lysed with 20% Triton-X 100 and diluted 33X with NaCl-saturating buffer or NaCl-free buffer to find out the dye encapsulation efficiency. (b) Proteoliposomes and control are each treated with NaCl-saturating and NaCl-free buffers to find out the change in fluorescence intensity. (c) The difference in fluorescence intensity for different samples in (a) and (b). Lysed control: red, lysed NaChBac: green, control: blue, NaChBac: purple. 45

Figure 4.1. Equations 4.10 and 4.11 are used to simulate the current and voltage going through the planar bilayer as it charges from 0 to 100 mV holding potential. The values used in this simulation was under the assumption that the BLM's capacitance is 100 pF, its resistance is 100 GΩ, and the electrode and buffer resistance is 10 Ω. (a) The voltage passing through the bilayer with respect to time (b) the current passing through the bilayer with respect to time..... 52

Figure 4.2 Optimization of perfusion condition for complete buffer exchange. (a) Fluorescence Intensity of 1 μM SG in 20mM Tris-Cl pH 7.4 buffer with 0, 5, and 150 mM NaCl using PTI fluorometer. (b) Fluorescence of 1 μM SG in the exchanged buffer when 150 mM NaCl is exchanged with distilled water. Only one single experiment was performed..... 57

Figure 4.3. Macroscopic current recording of NaChBac under varied buffer conditions. (a) Top panel: example of voltage step (5 s at -120 mV followed by 5 s at +60 mV) that is used for the recording of (a) and (b). Bottom panel: the current trace under 150/150 mM NaCl. At -120 mV, the channels deactivate at around 3.7s and at +60 mV, the channels activate almost instantly. (b) A zoom of the dotted blue box from (a) showing opening events in individual channels. (c) The single channel I-V plot obtained from macroscopic current recording. Buffer conditions are as below: 30/30 mM NaCl (blue dots); 30/150 mM NaCl (red squares); and 150/150 mM NaCl (green triangles). Unitary channel conductance is summarized in Table 4.2. This was found using peak currents at various step potentials (mean ± S.E.M., n = 40–100 events).... 63

Figure 4.4. Inhibition of NaChBac by lidocaine N-ethyl bromide. (a) Top panel: voltage protocol used in this experiment. Bottom panel: 4 out of the 40 current traces from NaChBac channel recording before any addition of drug (4 mM lidocaine N-ethyl bromide). (b) Zoom-in of the third current trace from (a) which shows two conducting levels (L1 and L2). (c) Average current trace. Black: before any drug addition (i.e. control), red: after the addition of drug in the cis chamber, blue: after the addition of drug in cis and trans chamber, grey: after removal of drug from the cis chamber. Each current trace is the average of 40 recordings. 67

Figure 4.5. Single channel current recording of NaChBac. (a) Voltage protocol used for the measurement. The channel was undergone a voltage protocol of -80 mV for 0.2 s, followed by a step voltage at +35 mV for 10 s before the voltage is set back to -80 mV for 0.8 s. (b) A representative trace of the recording. Three conducting levels are observed. (c-e) Zoom-in image of each of the three conducting sub-states. The experiment was repeated three times and the conductance were summarized in Table 3.3. 69

Figure 4.6. Single channel recordings with holding potentials from +80 to -80 mV in 5 mV increments. No data point displayed means no current events were found in that particular holding potential. (a) I-V plot in the absence of lidocaine N-ethyl bromide. While L1 (red square) opened in both positive and negative holding potentials, L3 (green triangle) and L2 (blue diamond) open less at lower potentials. (b) I-V plot of the same NaChBac in (a) in the presence of 4 mM lidocaine N-ethyl bromide in the cis

chamber. The presence of the inhibitor increases the observation of channel opening to L2 and 3 states, particularly at negative holding potential. 70

Figure 4.7. Overloading the SDS PAGE gel to look for contaminants. 74

Figure 4.8. Conductance of tag-free NaChBac and 6His-NaChBac using peak single channel currents found by macroscopic current recording. (a) Exemplary current trace for tag-free NaChBac recorded at +60 mV. O denotes the transient opening of an individual channel, while C denotes the baseline. (b) Exemplary current trace for 6HIS-NaChBac at +60 mV. (c) I-V plot obtained from opening event analysis. The 6His-NaChBac (red square) and tag-free NaChBac (blue diamond) have similar conductance (76 pS and 77 pS, respectively). One measurement was performed for each protein. . 77

Figure 4.9. Activation curve of NaChBac. (a) Voltage protocol used to obtain the activation curve. Protein was first held at -120 mV before switching to various activation step voltages (+20 mV, 0 mV, -10 mV, -15 mV, -20 mV, -25 mV, -30 mV, -40 mV, -50 mV, and -60 mV as labelled by black, red, green, blue, turquoise, pink, yellow, dark yellow, dark blue, and dark purple, respectively). A deactivation voltage of -120 mV was applied subsequently. The current traces shown are the average current traces after the voltage protocol is applied . (b) The activation curve of NaChBac which was found by plotting the current at 150 ms after switching back to the holding voltage potential of -120 mV. The current was plotted using I-V curve and fitted using the 2-state Boltzmann function as discussed in the context. 80

Figure 4.10. All point current histograms analysis for bi-ionic conditions for KCl and CaCl₂. I-V curve for NaChBac (a) 150/150 mM NaCl/KCl and (b) 150/150 mM NaCl/CaCl₂. Probability density function for CaCl₂ at (c) -60 mV and (d) +60 mV. (e) Open probability for KCl (blue diamond) and CaCl₂ (red square) bi-ionic conditions. Similar experiments were repeated three time and the result summarized in Table 4.5.
 83

Figure 4.11. Voltage ramp under asymmetrical buffer condition. An overlap of 100 current traces when voltage ramps from -100 mV to 100 mV in 2 s are shown in dark lines. (a) Bi-ionic buffer with KCl in the trans side of the bilayer and NaCl in the cis side. A representative individual trace showing no K⁺ conductance is highlighted in grey. (b) Same data set as (a), with the average highlighted in grey. (c) Bi-ionic buffer with CaCl₂ in the trans side of the bilayer. A representative individual trace showing no K⁺ conductance is highlighted in grey. (d) Same data set as (c), with the average trace highlighted in grey. Arrow head indicated the reversal potential obtained from I-V plots.
 85

Figure 5.1. Normalized scattering light intensity is plotted with respect to the change in the volume for vesicles with radius of 50 and 400 nm at 400 nm incident light.
 93

Figure 5.2. (a) A schematic diagram of the stopped-flow spectroscopy (b) Normalized scattering light intensities when NaChBac vesicles and control samples are mixed with 250 mM NaCl, 20 mM Tris-Cl, pH 7.2 (c) the NaChBac vesicles changing

from isotonic to hypertonic solution (d) Normalized scattering light intensities when NaChBac vesicles and control samples are mixed with 250 mM KCl, 20 mM Tris-Cl, pH 7.2..... 95

Figure 5.3. Normalized scattering light intensities when NaChBac vesicles and control samples are mixed with a hypertonic buffer. 98

Chapter 1 Introduction

NaChBac is a voltage-gated Na^+ channel from *Bacillus haloduran*. Studying this protein could help find strategies for removing bacterial biofilms, which is a bacterial community that is attached onto a surface. Biofilms are harmful in hospital settings and are difficult to remove from surfaces, thus presenting a challenge to the important objective of maintaining sterile environments where they are needed the most. Bacteria resistant to antibiotics and other currently ineffective sterilizations techniques are a growing concern and it is crucial that this is combatted by expanding the biomedical toolkits. Recently, bacteria in biofilms have been shown to rely on ion channels for communication and coordination (Prindle et al., 2015). Therefore, studying NaChBac may lead researchers to find innovative antibiotics and strategies that could disrupt bacteria in biofilms from communicating effectively.

NaChBac could also be used for desalinization. Current electrodialysis techniques allow for the desalinization of water by applying an electric potential difference through sodium and chloride ion permeable membranes. Although this technology is already used, its efficiency can yet be improved by reducing the back diffusion found in the ion permeable membranes (Rottiers, Ghyselbrecht, Meesschaert, Van der Bruggen, & Pinoy, 2014). Since NaChBac has an outward rectifying behavior, i.e. the channel passes current more easier from the outside than the inside (Ren et al., 2001), incorporating NaChBac into the membranes used in electrodialysis could improve this technology's desalination efficiency.

This thesis work is part of a larger project at Ingenuity Lab which is located in University of Alberta and under the direction of Dr. Carlo Montemagno. In this project

researchers seek to reconstitute the electrophysiological phenomenon known as action potential in an artificial system. Action potentials happen in excitable cells such as neurons and cardiac muscle cells when they generate electrical signals that code physiological messages in response to external or intrinsic stimuli. The process of action potential is well studied now. It involves the following steps in sequence: (1) a stimulus that depolarizes the cell membrane potential; (2) depolarization above the threshold potential triggers activation of voltage-gated sodium channels (Na_Vs) which allows further depolarization through influx of ionic sodium (Na^+); (3) sequential inactivation of Na_Vs and activation of voltage-gated potassium channels (K_Vs) which mediates out-flux of ionic potassium (K^+), both repolarizing the membrane; (4) K_Vs deactivates and at the cost of adenosine triphosphate (ATP), a $\text{Na}^+\text{-K}^+$ ATPase transports K^+ and Na^+ across the membrane against their electrochemical gradients to re-establish the resting membrane potential. The goal of the project is to develop and create next generation materials that are sentient with respect to the local environment, and to establish a model neuronal system for exploring the foundation of self-organized functional behaviour. The first step to achieve an artificial neuron system is to obtain purified protein of the ion channels and $\text{Na}^+\text{-K}^+$ ATPase with well-characterized activities. This thesis work thus focuses on the *in vitro* reconstitution of NaChBac and its functional characterization when the protein is in artificial lipid bilayer environment.

1.1 Hodgkin and Huxley's model on electrical current passing cell membrane

The mathematical model of the action potential mechanism was first developed in 1952, by studying the electrical signals in the squid giant axon (Hodgkin & Huxley, 1952a). Hodgkin and Huxley hypothesized that neurons act like technical electronic circuits and the electrical signals are generated by ionic current passing through proteins on the cellular membrane and has proposed a model to mathematically describe the function of the cellular membrane and voltage-gated ion channels.

In Hodgkin and Huxley's model, the cellular membrane can be regarded as a capacitor with a capacitance of C_m . The current passing through the membrane (I_m) is described as:

$$I_m = C_m \frac{dV}{dt} \quad (1.1)$$

The conductance of the sodium channels, g_{Na} , is described as:

$$g_{Na} = \bar{g}_{Na} m^{P_m}(t; V) h^{P_h}(t; V) \quad (1.2)$$

Where \bar{g}_{Na} is the maximum conductance for a sodium channel, m is the activation open probability of one gate, h is the inactivation open probability of one gate, P_m is the number of activation gates, and P_h is the number of inactivation gates. To further explain, m^{P_m} would be the probability of all activation gates open. P_m and P_h were obtained empirically by Hodgkin and Huxley. In addition, they also proposed that Na_V s has 3 activation gates and 1 inactivation gate (*i.e.* $P_m = 3, P_h = 1$), based on experimental data.

The conductance of the potassium channels, g_K , is described with the following equation:

$$g_k = \bar{g}_k n^p(t; V) \quad (1.3)$$

Where \bar{g}_k is the maximum conductance for a potassium channel, n is the activation (open) probability of one gate, and p is the number of gates in a potassium channel. Hodgkin and Huxley empirically found that the potassium channel has 4 activation gates ($p = 4$).

Therefore the total current through a membrane containing Na_V s and K_V s can be described as:

$$I_{total} = C_m \frac{dV}{dt} + g_{Na}(V_m - V_{Na}) + g_K(V_m - V_K) \quad (1.4)$$

where V_{Na} and V_K are respectively the reversal potential of the Na^+ and the K^+ .

As the parameters for the conductance of the ion channels in Equation 1.4 are empirically fitted with experimental data obtained from the squid giant axon expressing native ion channels (Hodgkin & Huxley, 1952b), action potential reconstruction in artificial neurons also needs to be characterised experimentally. Thanks to modern biotechnology and electrophysiology, it is possible to obtain purified ion channels and reconstitute them into an artificial lipid bilayer for single channel current study. The experimental data generated by studying ion channels in planar bilayers in house will help us refining the Hodgkin and Huxley model on an artificial neuron model. Once the model is refined, it is possible to simulate an artificial neuron and optimize the (ion) concentrations for extracellular and intracellular solutions so that the membrane is at the desired resting potential and the ion channels can function cooperatively.

1.2 Voltage-gated ion channel and NaChBac

Researchers believed Na_v s only exist in eukaryotes and so it was surprising to first discover them in *Bacillus halodurans*, a prokaryotic organism (Catterall, 2001; Ren et al., 2001). Its function is to transport Na^+ across the membrane, but its purpose in prokaryotes is not entirely clear; it is speculated that its role could be linked to communicating with surrounding prokaryotes (Prindle et al., 2015). Eukaryotic Na_v s have over 2000 amino acid residues with a large α subunit bound to few smaller β subunits (Catterall, 2001). In contrast, NaChBac, as other prokaryotic Na_v s that were discovered later, is a homotetramer with only 274 amino acid residues (Ren et al., 2001). Even though NaChBac contains notably less amino acid residues, it is able to retain the properties found in eukaryotic Na_v s such as Na^+ selectivity, voltage-dependent channel activation and inactivation, while their inactivation mechanism is different. During eukaryotic Na_v s inactivation, their N-terminal domain acts like a ball and chain to physically block ions from the intracellular side of the pore (Charalambous & Wallace, 2011). NaChBac's N-terminal domain is too short to produce a ball and chain to block the pore; instead, its pore undergoes a conformational change which is able to block ions from permeating through the pore (Charalambous & Wallace, 2011).

NaChBac was chosen as the Na_v to be used here because it can be easily overexpressed in *E. coli* and is well studied. This allows simple, rapid, and large-scale protein production when compared to producing a membrane protein in eukaryotes. As well, when purifying a bacterial (sodium) channel, researchers do not have to worry

about post-translational modifications that occur in eukaryotic cells. This means that it is easier to obtain larger quantities of voltage-gated ion channels in prokaryotic cells. To understand how NaChBac behaves in an artificial environment, the voltage-gated channel was purified from *Escherichia coli* (*E. coli*) and incorporated into black lipid membranes (BLMs) by fusing liposomes on the bilayer.

1.3 BLM technique

1.3.1 BLM device for membrane protein studies

The single molecule characterization of NaChBac in this thesis is done by incorporating the homotetrameric membrane protein into a BLM/planar lipid bilayer and studying the ions moving through the pore by controlling the transmembrane voltage and measure the resulting current. Such a lipid bilayer is named BLM because, when observed using a light microscope, the aperture holding the lipid bilayer appears to be black (Tien, Carbone, & Dawidowicz, 1966). BLMs are formed by applying a lipid sample over a small aperture submerged in saline-type solution. The lipid sample is usually previously dissolved in an organic solvent, prior to use, preferably decane. A BLM device is thus an apparatus that features a small area of planar lipid bilayer wherein membrane proteins can be inserted, and sensitive electronic devices that can control and measure voltage and current, respectively, in millivolts and in picoamps.

Incorporating proteins into a BLM is an established technique to characterize the behavior of membrane proteins that show conducting properties, i.e. ion channels. As

shown in Figure 1.1, a typical BLM setup includes the following components: amplifier, electrodes, salt bridges, and a sample holder that contains a trans and a cis chamber each designed for a fluid volume of 1 ml.

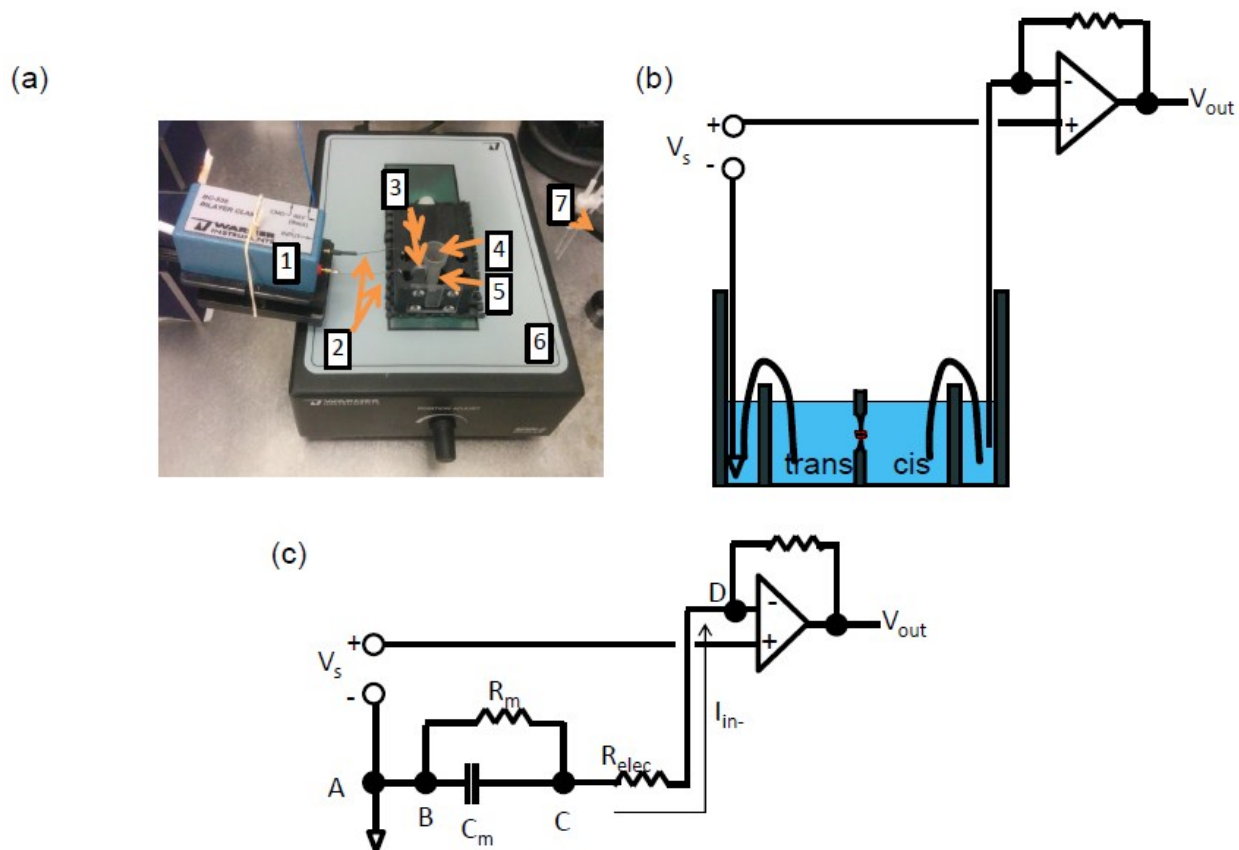


Figure 1.1. Illustration of a BLM workstation. (a) A picture of the BLM workstation used in this thesis. As labeled, it consists of a BLM headstage (1), Ag/AgCl electrodes (2), agar salt bridges (3), a trans chamber (4), a cis chamber (5), a stirring apparatus (6), and a perfusion setup (7). The above accessories are enclosed in a Faraday cage (not shown here), which serves to reduce electrical noise. (b) A schematic representation of the bilayer workstation. The reference electrode is in the trans chamber and the command electrode is in the cis chamber. (c) A simplified current schematic which

represents the bilayer workstation with a lipid membrane. V_s is the voltage source, R_m is the resistance due to the lipid membrane bilayer, C_m is the capacitance due to the lipid membrane bilayer, R_{elec} is the resistance due to the electrodes, I_{in-} is the current that is to be amplified, V_{out} is the voltage that is amplified from I_{in-} .

The trans chamber, also called the sample cup, refers to the chamber that is further away from the operating person and is the one that the reference electrode is connected to. As the trans side is the reference side, by convention, this side is considered to be the intracellular side of the cell membrane if a protein is inserted into the BLM. This chamber is removable and contains a small aperture for the lipids to be distributed across. The diameter of the aperture used in this thesis is 200 μm and the capacitance of the BLM formed across the aperture is usually 100-200 pF. Cis chamber refers to the chamber closer to the user and is considered as the extracellular compartment of the cell. The design of the sample chamber thus allows easy chemical and electrical access to both sides of the bilayer.

The amplifier is the most complex electronic element in a BLM device. The amplifier amplifies the electrical signal, sending it to an 8-pole Bessel filter where it then is analog signal is converted to a digital signal using an analog-to-digital converter (Digidata 1550, Molecular Devices) to be sampled into by the computer. A non-inverting amplifier is used in 'patch-clamp' techniques or BLM studies to amplify the pA current recording. In a non-inverting amplifier, the inverting voltage (V_{in-}) is connected to a ground voltage of 0 V and the non-inverting voltage (V_{in+}) will have a voltage that is equal to V_{in-} . As shown in Figure 1.2, an inverting amplifier will adjust the output voltage

(V_{out}) until the input signals V_{in+} and V_{in-} are equal to each other. The V_{out} is the amplified voltage of voltage difference between V_{in-} and V_{in+} and is amplified by increasing the gain to the amplifier.

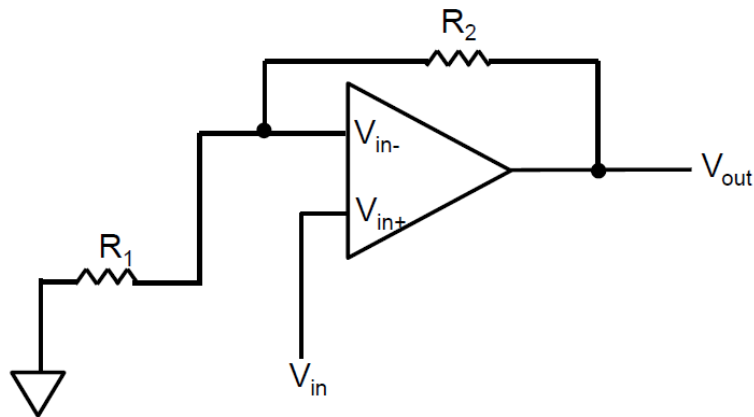


Figure 1.2. Schematic of an inverting amplifier.

When recording single channel properties, activation of the channel leads to a current step. The signal is usually filtered to improve its signal-to-noise ratio. But by filtering the recording, information encoded by the shape of the current step may get lost. The proper choice of filtering therefore reduces the loss of characteristic signal. An 8-pole Bessel filter is used in our setup as opposed to a 4-pole Bessel filter or a Butterworth filter since it can retain the step function characteristic of single channel current (Colquhoun & Sigworth, 1995). Using Butterworth filter tends to 'overshoot' the output signal. Although the 4-pole Bessel filter does not overshoot, the filtered current tends to have a longer time constant than an 8-pole Bessel filter, in that it takes longer to reach steady state current .

The electrodes used are unpolarized Ag/AgCl electrodes that allow current flow without producing an undesired double layer capacitance (Neuman, 1999).

The agar salt bridges are used to connect the Ag/AgCl electrodes that are immersed in concentrated KCl into both the cis and trans chambers. The high concentration of KCl ensures that the offset potential due to chloride ion concentration difference between the electrodes remains the same. The BLM setup is enclosed in a Faraday cage to reduce electrical noise and is positioned on a vibration-free table to minimize mechanical perturbation.

To incorporate NaChBac into the lipid bilayer, the vesicle fusion technique was used (Figure 1.3). For most membrane proteins, adding proteoliposomes to the bilayer generally has a higher chance of successful insertion than directly adding the membrane protein-detergent mixture (Darszon, 1983). Fusion of proteoliposome into the bilayer membrane will occur when the following two conditions are met: 1) the liposomes enter a hypertonic solution and swell while in contact with the planar membrane, 2) the solute concentration is less on one side of the planar membrane than the other so that the water will be forced to move to the side of the bilayer where the liposomes were inserted (Zimmerberg, Cohen, & Finkelstein, 1980). Accordingly, NaChBac liposomes with high concentration of solute are prepared and added to the cis chamber. The proteoliposome would swell under osmotic pressure and fuse into the bilayer, hence incorporating NaChBac into the bilayer.

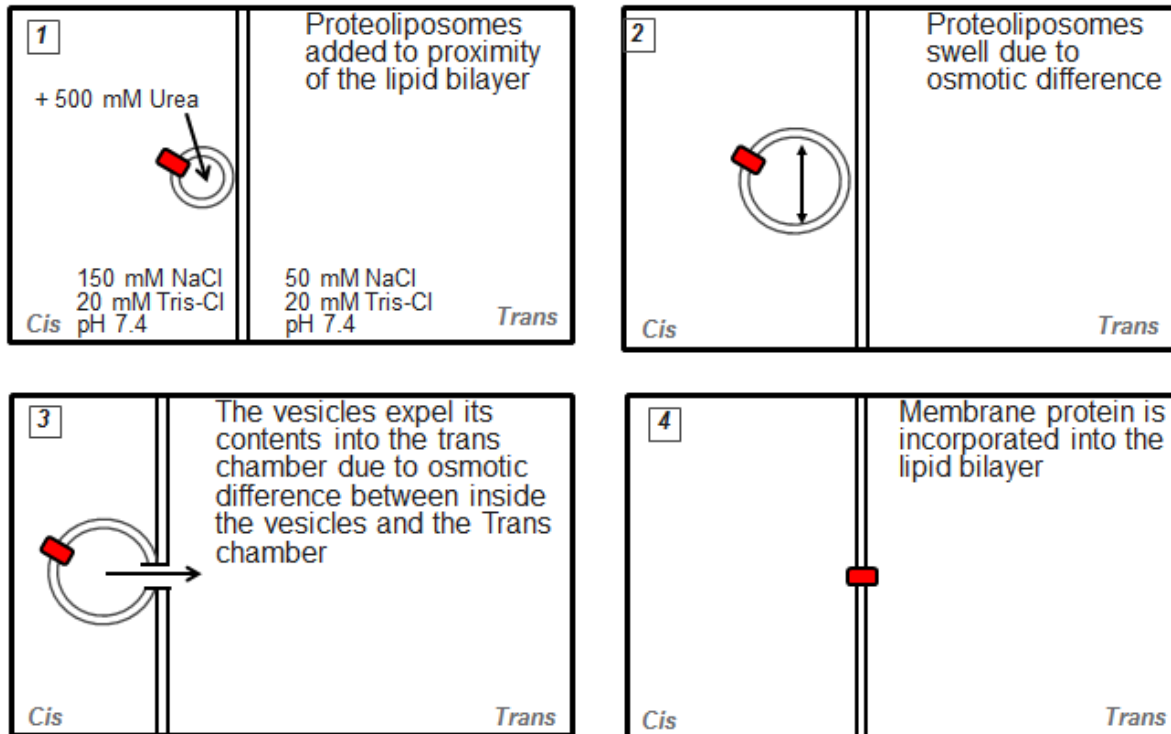


Figure 1.3. Schematic representation of the vesicles fusion onto the BLM.

1.3.2 Advantages and disadvantages of BLM

Compared to BLM current analysis, the other primary method of studying ion channel properties is patch-clamp. In this technique, a pipette, or the electrode, is pushed against the membrane of a cell that contains the protein of interest and a GigaOhm seal is formed and then the recording configuration such as whole-cell, excised or cell-attached patch is chosen (Marty & Neher, 1995). The tip of the pipette is formed by heating a capillary glass until it breaks apart and its diameter tends to be around a 1-3 μm (Kelly & Woodbury, 2003). Therefore the studying subject in patch-clamp, e.g. cells or giant liposomes, has to be larger than the size of the pipette. Patch-

clamp has been used to study membrane proteins expressed in many cell types, especially cardiac myocytes (Kelly & Woodbury, 2003), African green monkey kidney (vero) cells (Ren et al., 2001), and giant unilamellar liposomes (Riquelme, Lopez, Garcia-Segura, Ferragut, & Gonzalez-Ros, 1990). . Compared to studying proteins in planar bilayers in a BLM setup, patch-clamp has a higher signal to noise ratio and the protein is expressed in natural fashion on the cellular membrane (Kelly & Woodbury, 2003). The higher noise generated in BLM is due to the larger area of bilayer covering the aperture since its diameter is about 100X larger than the aperture of the patch-clamp electrode (Zakharian, 2013). In contrast, planar bilayers leave protein orientation to chance, and thus specific orientation is uncertain until otherwise determined.

The main advantage of using BLM is its higher success rate in incorporating a single protein onto the bilayer for electrical recording. Depending on patch clamp technique used (e.e. excised patch), it could possibly require more steps to obtain a single channel recording and this markedly decreases the chance of successful current recordings. When compared to patch-clamp, the BLM technique is particularly useful when it is desirable to alter membrane composition. To illustrate, in patch-clamp, one cannot modify the lipid composition of the plasma membrane of the cell that is used for the study; while for planar bilayers, the experimenter can easily manipulate the composition of the lipid membrane when preparing the lipid mixture for painting. This is useful when determining which membrane composition is required to incorporate stable proteins and for the protein to function properly (Cleverley, Geller, & Lenard, 1997; Kelly & Woodbury, 2003). The BLM technique also gives more flexibility in changing the

buffer environment of the lipid bilayer and the protein than patch-clamp techniques (Kelly & Woodbury, 2003). In patch-clamp, both intracellular and extracellular perfusion may be done, but when performing patch electrode perfusion, it must be done using a modified pipette (Maathuis, Taylor, Assmann, & Sanders, 1997). As a result, it is simpler to attempt the BLM approach. This is particularly true when an experimental design involves adding channel blockers into both sides of a membrane.

1.4 Scope of work and challenges

This thesis deals with the purification of NaChBac and the use of a fluorescence flux assay to examine its activity in Chapter 3. Particularly worth mentioning, the preparation procedure of proteoliposome was optimized and its preparation is critical for the rest of the thesis work. In Chapter 4, the single molecule behavior of NaChBac was studied using BLM, specifically its conductance, ion selectivity, and activation gating behaviour was studied. In Chapter 5, a scattered light-based flux assay was designed to examine NaChBac functionality and demonstrated its feasibility. NaChBac's functionality was verified using stopped-flow spectrometry when Na⁺ permeation into NaChBac proteoliposomes under osmotic pressure causes the liposomes to swell. Chapter 6 will conclude the given results found in this thesis work and will discuss potential future work and directions.

Though BLM is regarded as less skill-demanding than patch-clamp, it remains demanding. I started the project with equipment set-up, skill practice and procedure optimization. It was also very challenging to incorporate a single channel on the BLM

but after many trials a solution was found. Other problems involve compensating the capacitance current in single channel recordings to obtain the signal generated by NaChBac. I will discuss the troubleshooting and optimization in more detail wherever appropriate.

Chapter 2 Summary on Materials and Methods

2.1 Materials and instruments

- *E. coli* total lipid extract (Avanti Polar Lipids Inc)
- palmitoyl-oleoyl-phosphatidyl-ethanolamine (Avanti Polar Lipids Inc)
- palmitoyl-oleoyl-phosphatidyl-glycerol (Avanti Polar Lipids Inc)
- *E. coli* (BL21)
- pET28a vector (Novagen)
- Thrombin (GE Healthcare)
- Kanamycin (Thermo Fischer Scientific)
- Terrific Broth (TB)
- Luria broth (LB)
- Isopropyl β -D-1-thiogalactopyranoside (Sigma-Aldrich)
- Phenylmethylsulfonyl fluoride (Sigma-Aldrich)
- Ocyglucoside detergent (Sigma-Aldrich)
- N-dodecyl- β -D-maltoside (Sigma-Aldrich)
- DNase I (Thermo Fischer Scientific)
- Lysis buffer: 50 mM Tris, 150 mM NaCl, 2.5 mM MgSO₄
- Solubilization buffer: 50 mM Tris, 150 mM NaCl, 1% n-dodecyl- β -D-maltoside, pH 8.0
- Wash buffer: 50 mM Tris, 150 mM NaCl, 0.1% DDM, 20 mM imidazole, pH 7.4
- Elution Buffer: 50 mM Tris, 150 mM NaCl, 0.1% DDM, 300 mM imidazole, pH 7.4

- Sonication hydration buffer: 2 mM β -mercaptoethanol, 20 mM Tris-Cl, pH 7.4. 50 μ l of 200 μ M SG in 20 mM Tris-Cl (pH 7.4)
- Sodium Green Cell impermeant (Thermo Fisher Scientific)
- Fluorescent flux assay hydration buffer: 40 μ M Sodium Green, 20 mM Tris-Cl, pH 7.4
- Fluorescent flux assay salt buffer: 130 mM NaCl, 20 mM Tris-Cl, pH 7.4
- Fluorescent flux assay no salt buffer: 0 mM NaCl, 20 mM Tris-Cl, pH 7.4
- Fluorescent flux assay lysis buffer: 20% Triton-X100, 130 mM NaCl, 20 mM Tris-Cl, pH 7.4, or 20% Triton-X100, 0 mM NaCl, 20 mM Tris-Cl, pH 7.4
- BLM hydration buffer: 500 mM Urea, 150 mM NaCl, 20 mM Tris-Cl, pH 7.4
- BLM fusion buffer: 150 mM NaCl (cis), 50 mM NaCl (trans), 20 mM Tris-Cl, pH 7.4
- BLM bi-ionic buffer: 150 mM NaCl (cis) 150 mM KCl (trans), 20 mM Tris-Cl, pH 7.4 or 150 mM NaCl (cis) 150 mM CaCl₂ (trans), 20 mM Tris-Cl, pH 7.4
- Light Scattering Stopped Flow Spectroscopy hydration buffer: 500 mM Glycine, 20 mM Tris-Cl, pH 7.4
- Light Scattering Stopped Flow Spectroscopy dilution buffer: 250 mM NaCl, 20 mM Tris-Cl, pH 7.4
- Lidocaine n-ethyl bromide (Sigma-Aldrich)
- Lidocaine hydrochloride (Sigma-Aldrich)
- Nifedipine (Sigma-Aldrich)

- 0.2 µm cellulose acetate membrane syringe filter (Corning, New York, United States)
- Amicon Ultra-15 centrifugal filter unit, cutoff 10KD (Millipore, Billerica, United States)
- Ni-NTA-agarose beads (Qiagen, Hilden, Germany)
- Amersham ECL Western Blotting Detection Reagent (GE Healthcare, Mississauga, Canada)
- Superdex 200 5/150 (GE Healthcare, Mississauga, Canada)
- Bilayer Work Station (Warner Instruments, Hamden, United States)
- PTI Fluorescence Spectrophotometer (PTI, London, Canada)
- SX20 Stopped-Flow Spectrometer (Applied Photophysics, Surrey, United Kingdom)
- Zetasizer Nano ZS (Malvern Instruments, Malvern, United Kingdom)

2.2 Methods

2.2.1 Recombinant overexpression and purification of NaChBac

The cDNA coding for NaChBac was cloned from a NaChBac expressing *E. coli* strain (Patti & Montemagno, 2007) into a pET28a vector (Novagen) between the Nde I and EcoR I restriction sites. As a result, a hexahistidine tag is installed to the N-terminal of NaChBac, linked by a 10 amino acid spacer (Ser-Ser-Gly-Leu-Val-Pro-Arg-Gly-Ser-His). A protease cleavage site (Leu-Val-Pro-Arg-Gly-Ser) is included in the spacer, allowing the hexahistidine (6His-) to be removed by thrombin when required. The cDNA

sequence was confirmed by DNA sequencing service at the University of Alberta Molecular Biology Service Unit.

The expression plasmid is transformed into *E. coli* BL21(DE3). A fresh colony was grown in Luria broth (LB) with 30 µg/ml kanamycin for 13-16 h at 37°C. The cell culture was diluted 100X in Terrific Broth (TB) supplemented with 0.02 M glucose, 15 µg/ml kanamycin and the cells were allowed to grow at 37 °C until the optical density at wavelength of 600 nm (OD600) reached 1.0. The cells were induced by the addition of Isopropyl β-D-1-thiogalactopyranoside (IPTG) (final concentration 0.5 mM) and then were allowed to grow for another 4 h at 37°. The cells were harvested by centrifugation at 9000 g for 15 min and then the pellets were frozen at -20 °C. The pellet was resuspended in 1/40 culture volume of ice-cold lysis buffer (50 mM Tris, 150 mM NaCl, 2.5 mM MgSO₄) and additional 0.2 mM phenylmethylsulfonyl fluoride (PMSF), a protease inhibitor, and 2 µg/ml DNase I was added at use. The PMSF was used to prevent protease from hydrolysing the protein, and DNase I, an enzyme that cleaves DNA, was used to reduce the viscosity of the samples. The cells were lysed using French Press, a machine which moves the cells under high pressure through a narrow valve. The high change in pressure causes the cells to lyse (Kido et al., 2007). The sample was then centrifuged at 15,000 g for 30 min and the insoluble pellet was discarded. The supernatant was centrifuged for another 60 min at 140,000 g to recover the plasma membrane fractions. The membrane fractions were resuspended to 1/25 of original culture volume in solubilization buffer (50 mM Tris, 150 mM NaCl, 1% n-dodecyl-β-D-maltoside (DDM), pH 8.0). DDM solubilizes the NaChBac from the lipid

bilayer membrane. The lipid bilayer is not needed and so to remove it, the solution was centrifuged at 140,000 g for 45 min and the pellet was discarded. The soluble fraction, which contains the solubilized NaChBac along with other membrane proteins, was mixed with 1/5 volume of Ni-NTA-agarose beads (Qiagen) and was incubated with agitation at 4 °C overnight. The resin was washed with 60 bed-volume of wash buffer (50 mM Tris, 150 mM NaCl, 0.1% DDM, 20 mM imidazole, pH 7.4) by gravity flow. The protein was eluted using 5 bed-volume of elution buffer (50 mM Tris, 150 mM NaCl, 0.1% DDM, 300 mM imidazole, pH7.4). The eluted protein was then concentrated using Amicon Ultra-15 centrifugal filter unit (Millipore, cutoff 10KD) to <1/10 of original volume. The presence and purity of the purified protein is verified by SDS-PAGE.

To cleave off the 6His tag, purified NaChBac in phosphate saline buffer (PBS) was incubated with thrombin (GE Healthcare) at 4 °C for 12 h. For every milligram of protein, 5 units of protease were used. SDS-PAGE gel and Western dot blotting were used to confirm the cleavage. For the dot blotting procedures, an anti-6His goat antibody is used as primary antibody. An antigoat-peroxidase rabbit antibody was used as secondary antibody, and Amersham ECL Western Blotting Detection Reagent was used for signal development.

2.2.2 Liposome preparation and NaChBac incorporation

2.2.2.1 Optimizing dye encapsulation techniques for *E. coli* lipid

E. coli total lipid extract (Avanti Polar Lipids Inc.) was dissolved in appropriate buffer. For sonication and freeze-thaw methods, the lipid was dissolved in 2 mM β -

mercaptoethanol, 20 mM Tris-Cl, pH 7.4. 50 μ l of 200 μ M SG in 20 mM Tris-Cl (pH 7.4) was added 200 μ l of lipid. The final concentrations for the lipid is 32 mg/ml, and 40 μ M for the SG. In the sonication method, the sample was sonicated until it became translucent. In the freeze-thaw method, the sample was frozen in liquid nitrogen and then thawed in room temperature. For the direct hydration method, *E. coli* total lipid extract was dissolved with 40 μ M SG, 20 mM Tris-Cl, pH 7.4 at a final concentration of 32 mg/ml. 250 μ l of each of the samples prepared from the above methods were diluted into a total volumes of 27 ml and spun at 180,000 g for 1 h to remove excess dye. The supernatant was decanted and the pellet was resuspended to 1 ml in 20 mM Tris-Cl at pH 7.4.

2.2.2.2 Fluorescent flux assay

When performing the fluorescent flux assay, dye-containing lipid vesicles were prepared using the direct hydration method in which *E. coli* total lipid extract was dissolved with the buffer as listed in Table 2.1. The lipid concentration is 10 mg/ml. The sample was then freeze-thawed one cycle and then was solubilized by addition of concentrated DDM to a final concentration of 0.2%. The lipid solution was then extruded 10 X through a 0.2 μ m cellulose acetate membrane syringe filter (Corning®) to yield LUVs with diameters around 100 nm NaChBac was then added with a lipid to protein ratio of 100:1 (w/w). The incorporation of protein into the liposomes was done using the dilution strategy in which the mixture was diluted to a total volume of 27 ml so that the

concentration of DDM to below its CMC (0.07 mg/mL). The sample was centrifuged at 180,000 g for 1 h. The liposome pellet was resuspended with 20 mM Tris-Cl, pH 7.4.

2.2.2.3 BLM/stopped flow spectroscopy

E. coli total lipid extract and oylglucoside (Sigma-Aldrich) were dissolved in hydration lipid buffer (Table 2.1) with final concentrations of 20 mg/ml and 14.5 mg/mL, respectively. The lipid solution was subjected to the same freeze-thaw cycle three times in order to increase the homogeneity and the trapping efficiency of the liposomes (Mayer, Hope, Cullis, & Janoff, 1985; Szoka & Papahadjopoulos, 1980). The lipid solution was then extruded as aforementioned.

The NaChBac proteoliposomes were prepared using the detergent-assisted dilution method as explained in Section 3.1.1 (Jean-Louis Rigaud & Lévy, 2003). In the detergent-assisted method, NaChBac protein was added to the liposome sample with a protein to lipid ratio of 3000:1 (wt/wt) for BLM experiments and 50:1 and 100:1 for stopped flow spectroscopy experiments. The solution was then sonicated for 10 seconds to allow the protein to mix uniformly throughout the sample. The sample was then diluted so that the octylglucoside concentration in the sample is below its CMC (4.9 mg/mL) which allows the NaChBac to enter the liposome's membrane bilayer (Jean-Louis Rigaud & Lévy, 2003). The samples are diluted to up to 27 ml so that it fills the ultracentrifuge tubes. The vesicle samples were then continuously mixed for 20 min in room temperature. The vesicles were centrifuged at 180,000 g for 1 h. The supernatant was removed and the pellet was resuspended in 10 ml lipid buffer. The final

concentration of the lipid varied from 0.5 mg/ml to 1 mg/ml depending on the preparation batch.

Table 2.1. Table of buffers used to hydrate liposome powder for each experiment.

Experiment	Buffer used in dissolving lipid powder
Fluorescent flux assay (Chapter 3)	40 μ M Sodium Green, 20 mM Tris-Cl, pH 7.4
BLM (Chapter 4)	500 mM Urea, 150 mM NaCl, 20 mM Tris-Cl, pH 7.4
Light Scattering Stopped- flow Spectroscopy (Chapter 5)	500 mM Glycine, 20 mM Tris-Cl, pH 7.4

2.2.3 Fluorescence flux assay with fluorometer

The procedure of sodium flux assay using SG is shown in Figure 3.3. In this experiment, 30 μ l of vesicle sample was diluted 33X into no-salt buffer (20 mM Tris-Cl, pH 7.4), or salt buffer (130 mM NaCl, 20 mM Tris-Cl, pH 7.4) and the fluorescence was measured on a PTI Fluorescence Spectrophotometer. An excitation wavelength of 475 nm and an emission wavelength (or range) of 510 to 580 nm were used for detection of the SG fluorescence. To find out the maximum fluorescence change of the encapsulated dye, vesicles were lysed with no-salt lysis buffer (20% Triton X-100, 20 mM Tris-Cl, pH 7.4) and salt lysis buffer (20% Triton X-100, 130 mM NaCl, 20 mM Tris-

Cl, pH 7.4), respectively. The fluorescence was recorded for each treatment and the difference was determined and is shown in Figure 3.3.

2.2.4 Perfusion of BLM chambers

Buffer exchange was done by gravity flow perfusion whenever necessary. Generally, the perfusion is done on the trans chamber. The reason is due to higher chance for it to break on the cis chamber.

2.2.5 Incorporation of protein onto BLM by vesicle fusion

The planar bilayer is formed by painting a mixture of palmitoyl-oleoyl-phosphatidyl-ethanolamine (POPE) and palmitoyl-oleoyl-phosphatidyl-glycerol (POPG) with a ratio of 3:1 (wt/wt) across the aperture on the sample cup. In this thesis, NaChBac protein was incorporated into the lipid bilayer that was painted on the aperture using the vesicle fusion technique. In the fusion technique (Figure 1.3), NaChBac containing liposomes are added into the cis chamber filled with a hypertonic solution where they begin to swell and fuse into the lipid bilayer (section 1.2.1). 0.5 μ l of diluted proteoliposome sample was added in close proximity to the planar lipid bilayer. After 5-10 min, a holding potential was applied and an observation of current spikes indicates successful fusion of the protein. If the baseline of the current is above 0 pA, it suggests that multiple proteins have been incorporated into the lipid bilayer. If no insertion happens in 10 min, a more concentrated sample is used.

2.2.6 Single channel recording using BLM

2.2.6.1 8-pole Bessel Filter

The Planar Bilayer Workstation (Warner Instruments) is used to record channel currents and filter the data online using an 8-pole Bessel filter at 1 kHz. During analysis, the data were further filtered to resolved small current amplitude. Since the data are filtered twice, the final cutoff frequency (f_c) can be calculated using the following equation (Colquhoun & Sigworth, 1995) and it ranged from 1 to 0.1 kHz:

$$\frac{1}{f_c} = \sqrt{\frac{1}{f_1^2} + \frac{1}{f_2^2}} \quad (2.1)$$

2.2.6.2 Single channel analysis

The current peaks that are plotted on the I-V graph were found using either single channel search or through all-point histograms. Both of these methods can be done using Clampfit v.10 software (Molecular Devices Inc). The current trace is selected by placing cursor 1 and cursor 2 between the interested current (Figure 2.1a). Then the current peaks found using Single Channel Search can be found in the menu: **Event Detection** → **Single Channel Search** (Figure 2.1b). In the Single Channel Search window, Level 0 is selected as the baseline current, and Level 1 is selected as the peak current. The update levels automatically box was checked, and the setting to ignore short level changes of less than 5 ms was selected, as well, the latency mode was selected to ignore 5 ms of initial duration.

Another way that current peaks are found is through all point histogram and finding the peaks of the distribution. All point histograms can also be converted into probability density histograms which are important in finding the open and close probability of a channel. The all point histogram in Clampfit v.10 can be selected in the menu: **Analyze** → **Histogram** (Figure 2.1c). Once the histogram menu window pops up, Normalize Histogram Area should be checked to convert the histogram to a probability density function. The area can be fitted by selecting *fitting function* icon () in the histogram window (Figure 2.1c). The Gaussian distribution with 2 terms was selected. The results such as the peak and the area can be found by clicking *results* icon () in the histogram window (Figure 2.1c). The difference in the peak will give the current peak amplitude and the area for each peak will give the probability for each peak.

Often more than one protein gets incorporated into the planar lipid bilayer and the area under the peak cannot be used for a single channel. Assuming that each channel in the bilayer opens independently, the probability of r channels opening at a the same time (P_r) can be described as (Colquhoun & Hawkes, 1995):

$$P_r(p_o; N) = \frac{N!}{r!(N-r)!} p_o^r (1 - p_o)^{N-r} \quad (2.2)$$

Where N is the total number of channels in the bilayer, r is the number of channels open at the same time, and p_o is the open probability of a single channel. Setting Equation 2.2 so that there are 0 channels opening at the same time ($r=0$), the closing probability (p_c) can be determined:

$$p_c = (1 - p_o)^N \quad (2.3)$$

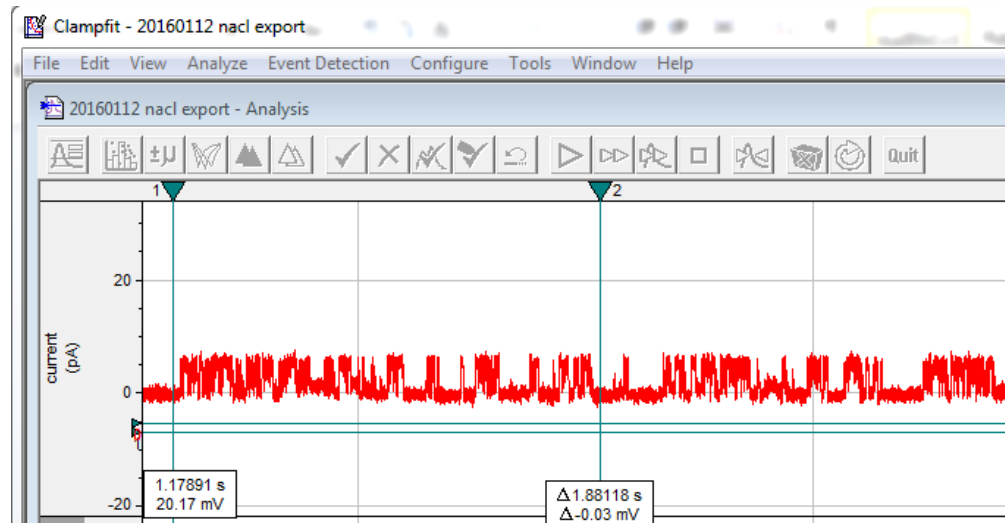
The closing probability can also be described as:

$$p_c = 1 - p_a \quad (2.4)$$

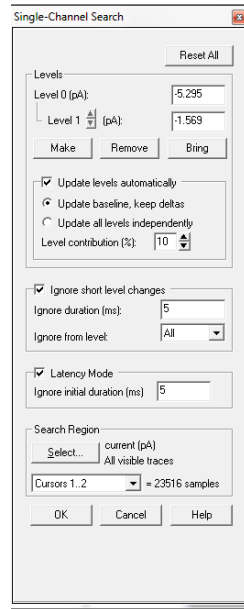
Where p_a is the probability that one or more channels open at the same time. Setting Equation 2.3 to equal to Equation 2.4, the open probability of one channel can be described as:

$$p_o = 1 - (1 - p_a)^{\frac{1}{N}} \quad (2.5)$$

(a)



(b)



(c)

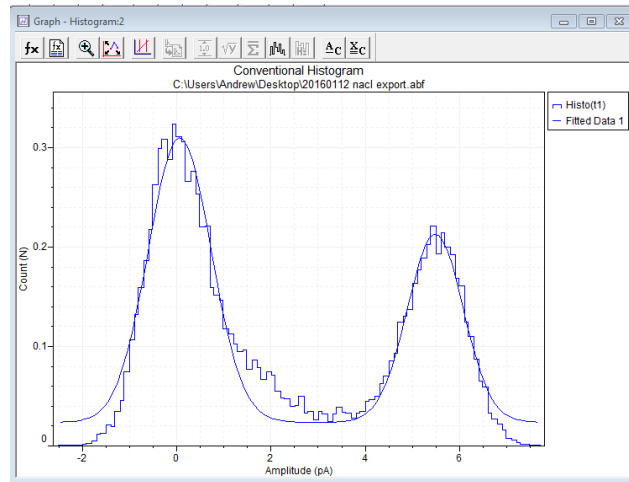


Figure 2.1. Using Clampfit, the peak currents to plot the I-V graph can be determined. (a) An example of a current trace recording (b) The Single Channel Search window (c) The All point histogram window.

2.2.6.3 Capacitance cancellation

Capacitance currents were cancelled when acquiring average current traces to determine the inhibition of NaChBac using lidocaine N-ethyl bromide (Section 4.2.2.2), This was done to show the section of average current traces that would have been hidden from the capacitance currents. 25 current traces were selected and averaged from each of the four ensemble average currents with the inactivated currents deleted from each of the traces (H. K. Lee & Elmslie, 1999).

2.2.6.4 Testing the inhibition of NaChBac using lidocaine N-ethyl bromide

4 mM of lidocaine n-ethyl bromide was added to the cis chamber. After the addition of the inhibitor, 5-10 min passed before acquiring current recordings. This was also done when adding the inhibitor to the trans chamber, and as well after perfusing the cis chamber with buffer to remove the inhibitor.

2.2.6.5 Measurement of E_{rev} for ion selectivity study

In the ion selectivity study, after NaChBac insertion the cis chamber was filled with 1 ml of 150 mM NaCl and the trans chamber was filled with 1 ml of 150 mM KCl or 150 mM CaCl₂. E_{rev} is used to determine the relative ion permeability using Equation 4.32 and Equation 4.36. There were two voltage protocols used to find E_{rev} (Figure 2.2).

- Bi-ionic protocol: The voltage were set to different holding voltages from -80 mV to +80 mV at 5 mV increments. The current peaks were then plotted against its holding voltage on an I-V plot. The E_{rev} is the x-intercept.
- Voltage ramp protocol: The voltage was ramped from -100 mV to +100 mV in 2 s. The E_{rev} is located at where the average current is at zero.



Figure 2.2. Voltage protocols used to find E_{rev} . (a) Bi-ionic protocol (b) Voltage ramp protocol.

2.2.7 Gel filtration chromatography and polydispersity measurement of liposomes

In Chapter 4, liposome sample was eluted through a gel filtration column (Superdex 200 5/150, GE Healthcare Life Sciences). The fractions collected from the column were collected and its size and polydispersity was measured using dynamic light scattering (DLS) (Zetasizer Nano ZS, Malvern Instruments). The sample's

concentration was adjusted by diluting the sample with sample buffer (500 mM Glycine, 20 mM Tris-Cl, pH 7.2) so that the attenuator factor is between 6 to 9.

2.2.8 NaChBac functionality by scattered light stopped-flow spectroscopy

A SX20 stopped-flow spectrometer (Applied Photophysics) with a 20 μ l optical cell and 1 ms dead time is used for the flux assay. The vesicle sample is rapidly mixed with equal volume of assay buffer (i.e. 250 mM NaCl or KCl, 20 mM Tris-Cl, pH 7.2, filtered and degassed), causing the corresponding ion to enter the vesicle. Light scattering was recorded at 90° to the incident light (400 nm). Under these conditions an increase in vesicle volume leads to a decrease in the signal. For all samples and conditions, at least 3 repeats, each of which is the average of at least ten traces, were recorded. Data were fitted to a monoexponential increase function and the initial rates (k) were calculated from the fitted equation. In the inhibition trial for NaChBac, the proteoliposome was pre-incubated with the known Na⁺ channel blocker lidocaine N-ethyl bromide (final concentration 1 mM) at room temperature for 10 min, followed by the aforementioned flux assay procedures.

Chapter 3 Protein Purification and Functional Characterization of NaChBac with
Fluorescence Flux Assay

3.1 Introduction

In this chapter, the purified NaChBac function is characterized using a dye-based flux assay. NaChBac was overexpressed in *E. coli* and purified using immobilized metal affinity chromatography (IMAC) based on a published report (Nurani et al., 2008). The molecular size and the purity of the NaChBac was verified using sodium dodecylsulfate polyacrylamide gel electrophoresis (SDS-PAGE), which is an electrophoresis method that separates biomolecules based on size. In SDS-PAGE, the negatively charged detergent SDS is used to denature protein into linearized structures and to give the protein a negative charge. A voltage is applied through the polyacrylamide gel and the proteins are separated in the gel by its electrophoretic mobility which is correlated to its molecular weight. NaChBac activity was determined by performing a flux assay using 'Sodium Green' (SG), a fluorescent Na⁺ indicator. In the flux assay, NaChBac was incorporated into SG-encapsulating lipid vesicles through a detergent-assisted dilution method. Three encapsulation techniques were tested (Szoka & Papahadjopoulos, 1980): (1) freeze-thaw, (2) sonication, and (3) direct hydration, to determine which of the three methods yields the best dye encapsulation efficiency. Subsequently, purified NaChBac is incorporated into dye-containing vesicles and demonstrated to be Na⁺-conducting.

3.1.1 Incorporation of membrane proteins into liposomes

When performing high throughput screening (HTS) of membrane proteins, it is common to incorporate them into artificial membranes such as lipid vesicles (i.e.

liposomes) to study its function. For example, researchers could incorporate membrane mitochondrial proteins into liposomes in order to observe their permeability for different ions or to observe their behaviour in different lipid compositions. Techniques on reconstituting membrane proteins into liposomes have been well established in literature. Rigaud and Lévy (2003) suggest that detergent-assisted proteoliposome formation is one of the most effective ways. In this method, a membrane protein, which has previously been solubilized by detergent, is mixed with pre-formed liposomes in the presence of detergent. The concentration of the detergent is important for efficient protein incorporation and can be optimized empirically based on the lipid composition and the species of the detergent. Complete removal of the detergent from the detergent-protein-liposome mixture is critical for proteoliposome that will be used for flux assay since residue detergent in the proteoliposome sample may compromise the integrity of lipid bilayer. Detergent removal can be done through dialysis, dilution, gel chromatography, or polystyrene beads methods, as will be discussed later. Alternatively, proteoliposomes can form through the use of sonication, freeze thawing, and organic solvents, but these procedures have been shown to degrade the membrane protein (Jean-Louis Rigaud & Lévy, 2003).

In the *dialysis method*, the detergent is added to the protein-liposome sample at a concentration above its critical micelle concentration (CMC). Above the CMC, the majority of the detergent molecules form micelles with the free monomers remains at constant concentration (i.e. the CMC). The detergent molecules cover the membrane protein's hydrophobic areas to prevent protein from aggregation. As the detergent

monomers diffuse out of the dialysis bag, the micelles break down into monomers, and the detergents on the protein surfaces starts to fall off, thereby forcing the membrane protein to inserted into the liposome. Dialyzing out the detergent monomers is slow and it could take up to a couple of days before the detergent is fully removed from the mixture. In the *dilution method*, the detergent is removed by diluting the mixture below its CMC which instantaneously forms proteoliposomes (Jean-Louis Rigaud & Lévy, 2003). Once diluted, the sample is centrifuged to collect the liposome pellet and it is then resuspended with detergent-free buffer. Another method is using gel filtration to remove the detergent from the mixture. As the mixture moves through the gel filtration column, the protein reconstitutes into the liposomes, and is separated from the detergent as the detergent micelles and the protein are smaller and therefore able to enter resin pores (Allen, Romans, Kercret, & Segrest, 1980; J.-L. Rigaud, Levy, Mosser, & Lambert, 1998). Gel filtration is generally not used due to the non-uniform protein incorporation (Jean-Louis Rigaud & Lévy, 2003). As well, after using gel filtration or dilution, trace amount of detergent still remains and so further steps may be required to completely remove detergent from the mixture. With the *polystyrene beads method*, beads are added to the protein-lipid-detergent mixtures. The beads adsorb the detergent from the solution which allows for the formation of proteoliposomes. Once the beads fully remove the detergent from the solution, it can be removed through centrifugation. It is disadvantageous to use biobeads if lipid concentration is important as it is possible for some of the lipids to be adsorbed onto the beads (Ollivon, Lesieur, Grabielle-Madelmont, & Paternostre, 2000).

3.1.2 Fluorescence flux assay

Pharmaceutical companies employ high throughput screening (HTS) of ion channels which uses either fluorescence dye or radioactive tracers to observe the ion flux into or out of the cell. In the fluorescence flux assay, researchers use a fluorescent ion probe such as SG and Fura-2, which fluoresce according to changes in the Na^+ or Ca^{2+} concentration (Xu et al., 2001). The dye is encapsulated into the cells and then the sample buffer is washed to remove any dye from the extracellular fluid. The studied ion is then added to the sample buffer to measure the ion's fluorescence change as it enters the cells. Researchers who use fluorescence assays can also detect the voltage change in liposomes through fluorescence resonance energy transfer (FRET), a mechanism that occurs when a donor chromophore and an acceptor chromophore molecule are close enough that donor chromophore is able to transfer energy to the acceptor chromophore (Pollok & Heim, 1999). In the case of HTS, a donor chromophore such as coumarin is inserted into the outer leaflet of the membrane and an acceptor such as oxonol, a negatively charged molecule, is added to the buffer solution. When the oxonol molecule is in close contact with the excited coumarin tagged phospholipids, the excited coumarin molecule would "donate" its energy to the oxonol molecule so that the oxonol molecule would fluoresce. If the liposome membrane potential hyperpolarises, oxonol will move towards the inner leaflet of the membrane. Much of the oxonol molecules will then be at far enough distances from the coumarin that the molecules in solution would experience a reduced fluorescence. The use of

fluorescent dyes is attractive when screening for drugs, but prone to misleading results if the molecule can influence the dye's emission (Xu et al., 2001). In these cases, radioisotope tracers could be used as its signal is not influenced by neighbouring molecules. Isotopes such as $^{86}\text{Rb}^+$ for K^+ channels and $^{22}\text{Na}^+$ for sodium channels are encapsulated into liposomes and its sample buffer is then washed to remove isotope tracer in extra cellular solution. The sample then is exposed to a possible drug and the radioactive flux outside of the cells is observed using a scintillation counter. The major drawback in using radioisotope tracers is it has lower time resolution than fluorescent assays, and is considered less safe (Xu et al., 2001).

3.2 Results and discussion

3.2.1 Recombinant overexpression and purification of NaChBac

NaChBac is the first prokaryotic Nav being discovered (Catterall, 2001). It has been shown that NaChBac can be readily overexpressed in heterologous systems such as *E. coli* and mammalian cells. Following published procedures (Nurani et al., 2008) and standard protein purification protocols, I was able to overexpress NaChBac in *E. coli* and purify the protein using protein chromatography. To facilitate the purification, an affinity tag (hexahistidine, 6His-) was introduced to the N-terminal of the protein sequence. The 6His tag can be removed by protease (thrombin) after purification. A yield of 2-4 mg of protein was obtained from 1 litre of bacterial culture. Figure 3.1a shows the SDS-PAGE of the purified protein. The calculated molecular weight of 6His-

tagged NaChBac is 33 kDa. The purified NaChBac (lane 3 in Figure 3.1a) appears as a major band around 28 kDa, with a minor band at around 120 kDa. The 28 kDa band corresponds to the monomer, while the faint band at ~120 kDa was thought to be a tetrameric assembly but later was found to be contaminant AcrB using mass spectrometry (see further discussion in Chapter 3). The two bands on the SDS-PAGE are consistent with previous literature (Patti & Montemagno, 2007), but it was reported that the ~120 kDa band is from NaChBac producing as a tetramer. The gel also confirms that the removal of the 6His tag in the thrombin treated sample (lane 2 in Figure 3.1a). NaChBac incubated with protease is roughly 25 kDa, slightly smaller than 6His-NaChBac. Moreover, the 6His tag removal is confirmed using dot blot (Figure 3.1b). Amersham ECL Western Blotting Detection Reagent was used to detect the secondary HRP labelled antibody which binds to the anti HIS-tag goat primary antibody. When comparing with Blot 2, Blot 1 contains minimum signal. This suggests that the secondary conjugate antibody was unable to find any HIS-tag to bind to which suggests that the HIS-tag was successfully cleaved off the NaChBac.

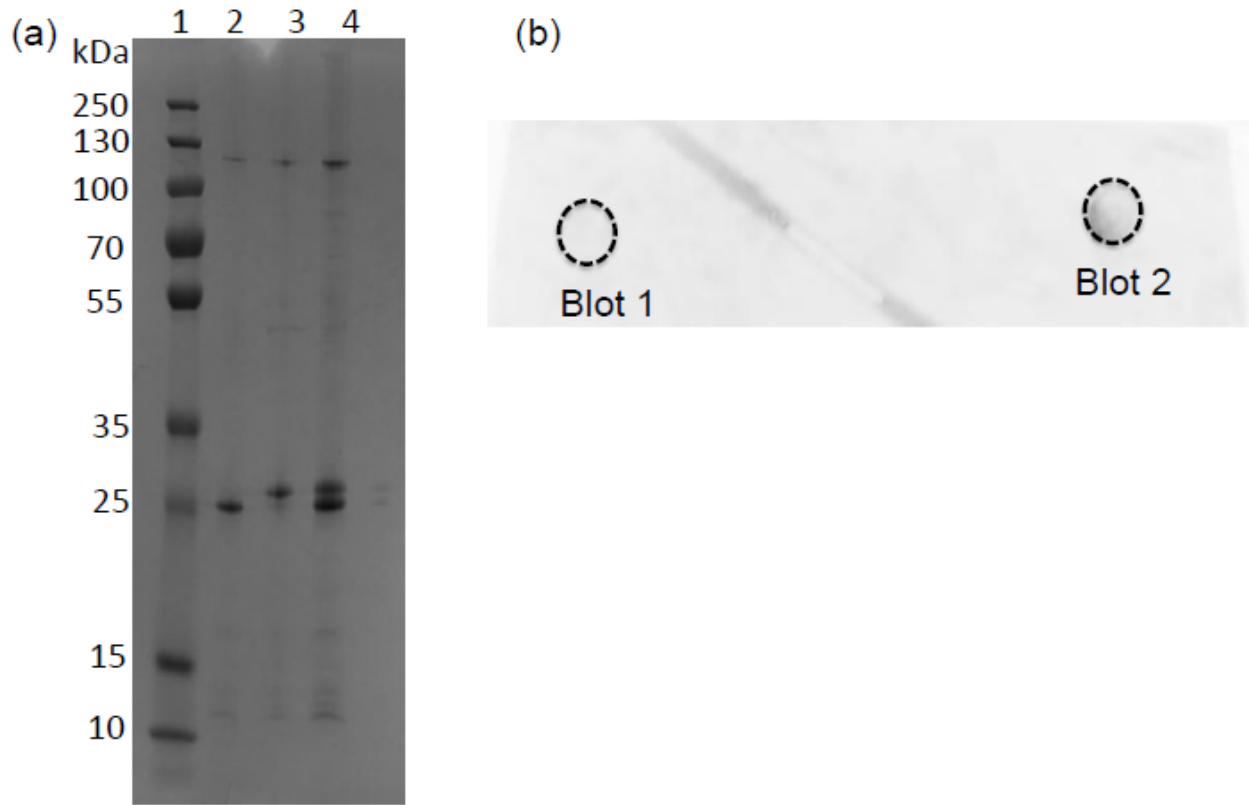


Figure 3.1. The HIS-tag of NaChBac was cleaved and verified using SDS-PAGE and dot blot test. (a) Pseudo-native SDS-PAGE gel of 6His-tagged and tag-cleaved NaChBac. Lane 1: protein standards (PageRuler Easy Plus, Thermo Scientific); lane 2: 6His-tagged NaChBac incubated with thrombin for 12 h; lane 3: 6His-tagged NaChBac without thrombin treatment; lane 4: mixture of both types of NaChBac. b) The dot blot test which tests for the 6His-tag on the NaChBac cleaved protein. 2 μ l of each sample at 50 μ g/ml was applied. Spot 1 is NaChBac after thrombin digestion and spot 2 is a positive control that contains KvAP with 6His-tag.

3.2.2 Encapsulation Efficiency

Next, the dye encapsulation efficiency of different liposome preparation methods was studied. The methods used include: (1) freeze thaw, (2) direct hydration, and (3) sonication. In both freeze-thaw and sonication methods, large multilamellar vesicles (LMVs) were preformed. In freeze-thaw, encapsulation of the dye occurs at the thawing step when the ice crystals formed during the freezing step disrupt the cell membrane and allow the SG dye to diffuse into the liposome (Costa, Xu, & Burgess, 2014). In sonication, the LMVs were sonicated in a cold water bath and they break down into smaller unilamellar vesicles (Szoka & Papahadjopoulos, 1980). During this transformation, the liposomes become permeable to water soluble molecules. Although in this study ice water bath was used during sonication LMVs below the lowest crystallization temperature (T_c) of the composing lipid has been known to increase defects in the membranes, thus increasing the encapsulation efficiency, and promote vesicle fusion and growth after the temperature goes above T_c (Szoka & Papahadjopoulos, 1980). In direct hydration, the lipid monomers self assemble in the drug solution (Szoka & Papahadjopoulos, 1980).

To find out the dye encapsulation efficiency, a salt treatment procedure was employed in which the liposome sample was diluted into a salt-saturated buffer (130 mM NaCl, 20 mM Tris, pH 7.4) and a salt-free buffer (20 mM Tris, pH 7.4), respectively, for fluorescence measurement. As the fluorescence intensity depends on both $[Na^+]$ and $[SG]$, the difference in the fluorescence spectra upon saturating salt treatment reflects

the concentration of SG. Accordingly, the fluorescence intensity change was determined by subtracting the fluorescence of vesicles that were treated with salt-free buffer from vesicles that were treated with saturating NaCl buffer (Figure 3.2). This fluorescence change is hence due to only the salt treatment and not due to the liposomes or the sample buffer. The dye-encapsulating vesicle was then lysed by introducing Triton X-100 to the sample (final concentration 0.97%) to release all the dye to the bulk solution (Epanand et al., 2003).

The SG fluorescence in the liposome samples display an increase and a blue shift upon the addition of NaCl (from 528 nm to 524 nm), and an increase and a red shift upon addition of Triton X-100 (from 528 nm to 542 nm). Unlysed liposomes that were treated with NaCl underwent a small fluorescence increase when compared to its control (i.e. SG-free liposome) (Figure 3.2a). This is probably due to either SG being trapped in the hydrophilic parts of the vesicle membrane, or more likely, due to residue SG that was left over from when the centrifuged sample was decanted in order to remove the dye. Previous studies confirms that Na^+ is impermeable to lipid bilayers due to its charge (Szoka & Papahadjopoulos, 1980). Accordingly, Na^+ should not be permeable to liposomes with integrated bilayer structure.

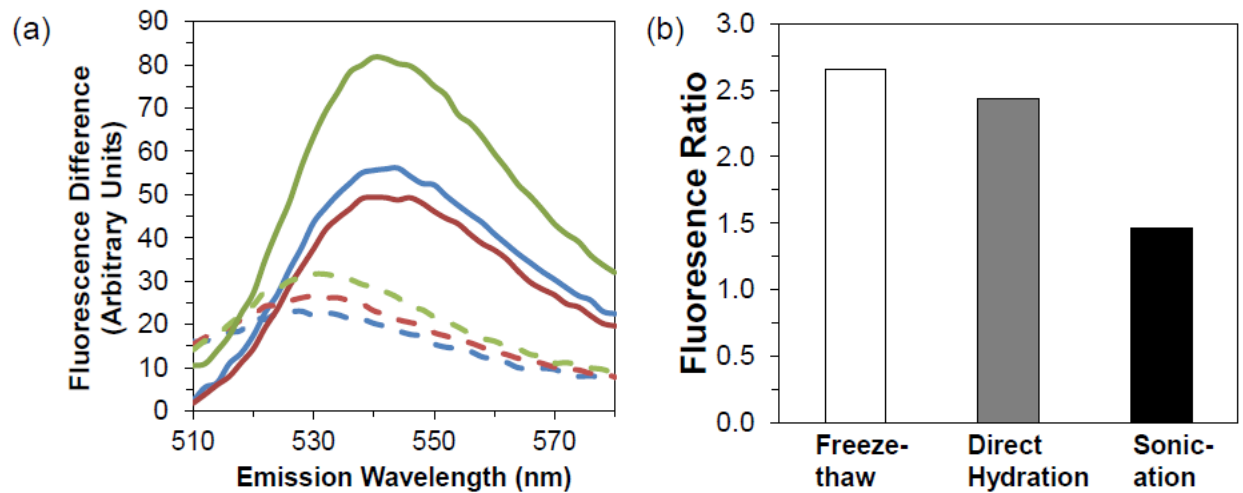


Figure 3.2. Fluorescence of Sodium Green (SG) in liposome samples prepared by different encapsulation techniques. (a) Difference in fluorescence spectra of the SG-containing liposome upon salt-treatment. Samples were prepared by sonication (red), direct hydration (blue), or freeze thaw (green) and tested without (dash line) and with (solid line) the presence of Triton X-100. (b) Ratio of the intensity change of the samples after and before lysis for each encapsulation method used.

The ratio of the fluorescence change upon salt treatment after and before lysis was calculated (Figure 3.2b) and used to compare the encapsulation efficiency of different methods since it quantifies the change that is due to encapsulated SG. Comparing the three encapsulation methods, the freeze thaw technique performed the best with the direct hydration method being a close second (Figure 3.2b). Freeze-thaw disrupts the membrane through ice crystal growth and allows the dye to diffuse into the membrane (Costa et al., 2014). In addition, freeze-thaw increases the trapping efficiency of liposomes by making the vesicles more unilamellar (Mayer et al., 1985). As

shown in Figure 3.2, sonicating the liposomes was the least efficient in encapsulating SG. It appears, freeze-thaw method causes more disruption in the membrane than sonication and allows more of the dye to diffuse through the membrane.

Based on the above result, a combination of direct hydration and freeze-thaw is used to prepare SG-containing vesicles for the protein functional assay.

3.2.3 Functional characterization of NaChBac with dye-based flux assay

In order to test NaChBac's functionality in liposomes, the protein is first incorporated into SG-containing liposomes using detergent-assisted method. When the proteoliposome is diluted into a salt buffer, influx of Na^+ through NaChBac will lead to increased fluorescence. In contrast, vesicle without NaChBac (i.e. control) will have minimum fluorescence change upon dilution into salt buffer as Na^+ has a very low permeability across the lipid bilayer. Maximum fluorescence change is again obtained by lysing the vesicle samples with Triton X-100 in the presence or absence of Na^+ .

As shown in Figure 3.3, NaChBac vesicles showed a bigger change in fluorescence intensity upon the salt treatment than the control does, suggesting that NaChBac vesicles are more permeable to Na^+ . To further confirm that the fluorescence increase observed in the NaChBac vesicles is the result of Na^+ permeability, I lysed the vesicles and found the fluorescence difference when it is in salt-free and salt-saturating conditions, respectively. The fluorescence difference correlates to how much dye is in the sample, and since the fluorescence difference of NaChBac vesicles and control vesicles upon lysis is similar (green and red line in Figure 3.3), this indicates the amount

of dye the vesicles encapsulated are similar. Hence the fluorescence change upon salt-treatment in the proteoliposome sample is due to Na^+ permeability through NaChBac.

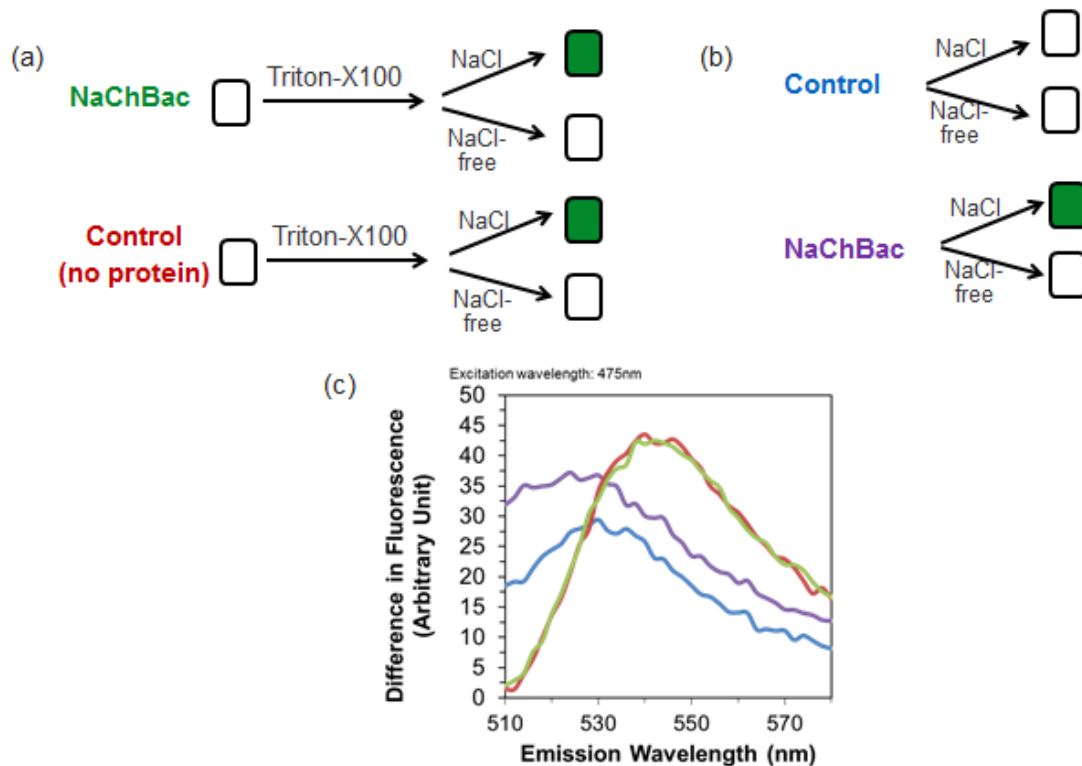


Figure 3.3. Schematic representation and experimental result of the fluorescence flux assay with SG. (a) The vesicle samples were lysed with 20% Triton-X 100 and diluted 33X with NaCl-saturating buffer or NaCl-free buffer to find out the dye encapsulation efficiency. (b) Proteoliposomes and control are each treated with NaCl-saturating and NaCl-free buffers to find out the change in fluorescence intensity. (c) The difference in fluorescence intensity for different samples in (a) and (b). Lysed control: red, lysed NaChBac: green, control: blue, NaChBac: purple.

3.3 Conclusion

Dye encapsulation methods, namely freeze-thaw, direct hydration, and sonication were studied, and they are listed in the order of encapsulation efficiency. Sodium Flux assay was prepared by combining freeze-thaw and direct hydration methods, encapsulating SG into the vesicles and then incorporated NaChBac using the detergent-assisted dilution method (Jean-Louis Rigaud & Lévy, 2003). In summary, the purified NaChBac protein reported in this thesis is permeable to Na⁺ when incorporated into lipid vesicles.

Chapter 4 Using Planar Bilayer Membranes to Characterize NaChBac

4.1 Introduction

NaChBac has six subdomains according to its hydropathy plot (Ren et al., 2001). The selectivity filter found in the pore region is at position 190-195 with the following amino acids sequence: leucine-glutamic acid-serine-tryptophan-alanine-serine (LESWAS) (Charalambous & Wallace, 2011). Its ion selectivity filter is important in allowing the permeation of the Na^+ through the ion pore by stripping its hydration shell (Zhang et al., 2012). Its ion selectivity comes from the fact that the Na^+ can enter towards the dehydration site closer than other ions which allows for it to use the least amount of dehydration energy (Eisenman & Horn, 1983). Changing the serine amino acid residue at position 195 to aspartic acid (LESWAS to LESWAD) loses NaChBac's ability to select among cations (Charalambous & Wallace, 2011). Changing serine 192 to aspartic acid (LESWAS to LEDWAS) or changing both serine 192 and serine 195 to aspartic acid (LESWAS to LEDWAD) changes the channel's selectivity to be more favourable to Ca^{2+} ions (Charalambous & Wallace, 2011). Eukaryotic ion channels undergo the ball and chain inactivation mechanism in which after channel activation, the N-terminus (the ball) blocks the pore from the intracellular side. This does not occur in NaChBac as its N-terminus is too short to block the pore; instead, the pore region aids in the inactivation gating of NaChBac and because of this, it is up to 100 times slower than the inactivation rates of eukaryotic sodium channels (Charalambous & Wallace, 2011). The activation of NaChBac depends on the highly-conserved arginine residues on the fourth transmembrane helix (Zhang et al., 2012), for example, Chahine et al.

(2004) substituting arginine 120 from the fourth subdomain to cysteine (R120C) shifts which shifted their NaChBac's activation half voltage from -24 mV to 11 mV.

NaChBac has been reported to have different conductance values when incorporated in a biological or artificial membrane. A patch-clamp study done in mammalian cells report a conductance level of 12 ± 1 pS (Ren et al., 2001), while other BLM studies reported NaChBac to have a single conductance between 106 or 120 pS (Saha et al., 2015; Studer, Demarche, Langenegger, & Tiefenauer, 2011). While NaChBac's gating behaviour has been studied in patch-clamp, it has not yet been reported using BLM. It is easier to study gating behaviour in patch-clamp than in BLM as the latter approach has larger capacitive currents that reduce the ability to study the first few microseconds of the current recording. This chapter describes my effort to study the conductance, ion selectivity, and gating behavior of NaChBac at single molecular level using BLM.

4.1.1 Capacitive current

In BLM data (and also patch-clamp data), there is generally capacitive current at the beginning of a voltage pulse. This can be explained in more detail when treating the system as a circuit diagram (Figure 1.1). The lipid membrane displays intrinsic capacitance and can be treated as a capacitor as shown in Figure 1.1b.

Assuming that the NaChBac is open, and the channel produces a constant current (i.e. the protein is viewed as R_m in Figure 1.1c), Kirchoff's Current Law (KCL) was used at node C to find the total current ($I_{in.}$) going through the inverting input.

$$I_{in-} = I_1 + I_2 \quad (4.1)$$

I_1 is the current running through the membrane resistance:

$$I_1 = \frac{V(t)}{R_m} \quad (4.2)$$

I_2 is the current traveling through the membrane capacitance.

$$I_2 = C_m \frac{dV}{dt} \quad (4.3)$$

Equation 4.3 and Equation 4.2 is plugged into Equation 4.1:

$$I_{in-} = C_m \frac{dV}{dt} + \frac{V(t)}{R_m} \quad (4.4)$$

Since node A is set to ground, V_C is the voltage experienced on the bilayer, so:

$$V(t) = V_C \quad (4.5)$$

R_{elec} , being the resistance from the electrode and the buffer, and given that the non-inverting voltage (V_s) equals to the inverting voltage (V_{in-}), the current (I_{in-}) passing through node C can be described by the following equation:

$$I_{in-} = \frac{V_s - V}{R_{elec}} \quad (4.6)$$

Equation 4.6 was then substituted into Equation 4.4 and given that the voltage changes in a pulse like manner, a Heaviside function can be used to describe the voltage change going through the bilayer work station at time b .

$$u(t - b) \frac{V_s}{C_m R_{elec}} = \frac{dV}{dt} + \frac{V}{C_m R_{eq}} \quad (4.7)$$

Where

$$R_{eq} = \frac{R_{elec} R_m}{R_{elec} + R_m} \quad (4.8)$$

Laplace transform was used to solve for the differential equation and for simplicity in solving the equation, $V(0)$ equal to 0.

$$F(s) = \frac{V_s e^{-bs}}{C_m R_{elec} s \left(s + \frac{1}{C_m R_{eq}} \right)} \quad (4.9)$$

Inverse Laplace transforming Equation 4.9 will get:

$$V(t) = u(t - b) \left[\frac{V_s R_m}{R_{elec} + R_m} \left(1 - e^{-\frac{t-b}{C_m R_{eq}}} \right) \right] \quad (4.10)$$

Adding Equation 4.10 into Equation 4.4 will show the current that is passing through the lipid bilayer with respect to time:

$$I_{in-} = u(t - b) \left[\frac{V_s}{R_{elec} + R_m} + \left(1 - \frac{R_{eq}}{R_m} \right) \frac{V_s}{R_{elec}} e^{-\frac{(t-b)}{C_m R_{eq}}} \right] \quad (4.11)$$

Using Equation 4.11, when a voltage step is applied (V_s is held constant), the voltage passing through the membrane has an exponential decay (increasing form). This creates a current spike, known as membrane capacitive current, which decays in an exponential manner. From Equation 4.11, the bilayer capacitance and resistance, and the electrode/buffer all affect the capacitance current's decay rate.

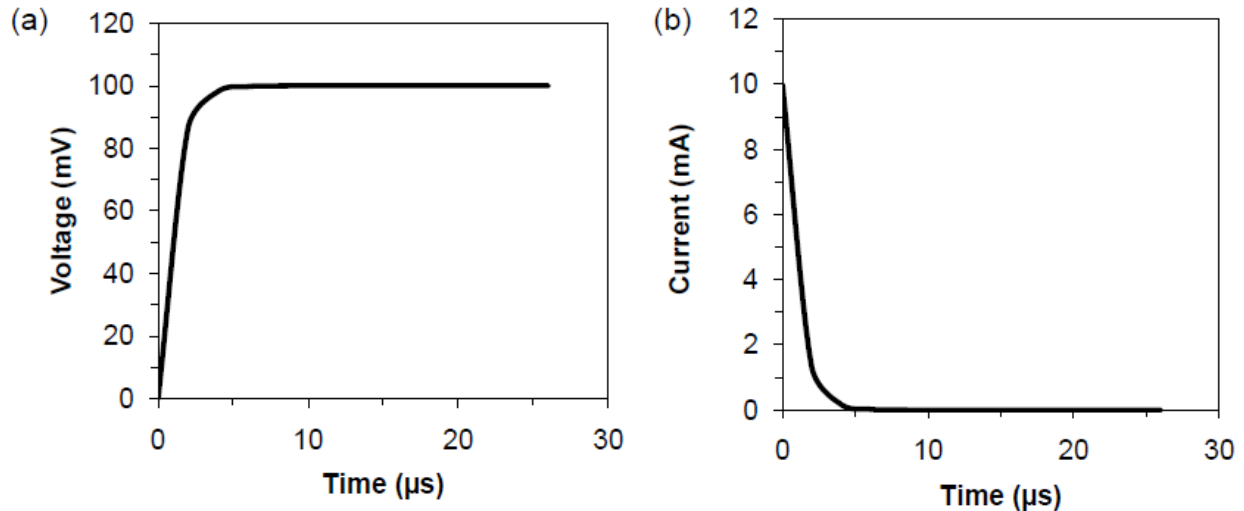


Figure 4.1. Equations 4.10 and 4.11 are used to simulate the current and voltage going through the planar bilayer as it charges from 0 to 100 mV holding potential. The values used in this simulation was under the assumption that the BLM's capacitance is 100 pF, its resistance is 100 G Ω , and the electrode and buffer resistance is 10 Ω . (a) The voltage passing through the bilayer with respect to time (b) the current passing through the bilayer with respect to time.

A simple solution to minimize the effect of membrane capacitive current on single channel recording is to perform capacitance cancellation by adding a capacitor into the circuit and applying a voltage to generate a charging current with opposite sign to I_s . The BC-535 bilayer clamp amplifier (Warner Instrument) that is used in our setup has a build-in capacity compensation circuit that can provide a maximum capacitance compensation of 500 pF.

Another technique that can be combined with capacitance cancellation is lowering the electrode series resistance compensation. This decreases the electrode

resistance, but it will also increase the voltage around the membrane bilayer (Marty & Neher, 1995). If the electrode resistance is not determined correctly, this will lead to the incorrect voltage being applied to the membrane. To cancel out the remaining capacitance currents, the user must obtain a control current which has no current steps due to the protein channel. This control current is then cancelled with the experimental current which then only current due to the channel will be displayed.

4.1.2 Permeability of K^+ and Ca^{2+}

Previous studies have established that NaChBac is an INav with high Na^+ selectivity when expressed in mammalian cells (Ren et al., 2001). BLM was used to study the ion selectivity of purified NaChBac protein. A lipid bilayer incorporating NaChBac can thus be treated as a potentially Na^+ selective membrane. Theories on NaChBac's selectivity and permeability towards K^+ and Ca^{2+} can now be applied to study the system relative to Na^+ . Its selectivity to K^+ and Ca^{2+} was determined by the equation the Goldman equation (Goldman, 1943). Goldman assumed the two things that affects the ion's flux (j) in a membrane is diffusion and the electric field which is shown in the following equation:

$$j_A = -D_A \left(\frac{d[A]}{dz} - \frac{n_A F E_{rev}[A]}{RTL} \right) \quad (4.12)$$

Where D_A is the diffusion coefficient expressed in m^2/s , $[A]$ is the ion concentration expressed in mol/l , F is the Faraday constant which is $96,485.3 \text{ s}\cdot\text{A}/\text{mol}$, E_{rev} , which is expressed in volts, is the reversal potential required for no net movement of ions between a membrane which is expressed in volts, n_A is the valence charge of the ion, R

is the gas constant 8.314 J/K/mol, T is the temperature in K, z is the distance of the ion movement, and L is the thickness of the membrane in m.

The equation is simplified by substituting the following variables as μ .

$$\mu = \frac{FE_{rev}}{RT} \quad (4.13)$$

The differential equation in Equation 4.12 is solved by separation of variables:

$$\int_{[A]_{in}}^{[A]_{out}} \frac{d[A]}{-\frac{j_A}{D_A} + \frac{n_A \mu}{L} [A]} = \int_0^L dz \quad (4.14)$$

And 'u' substitution is used to solve the integral

$$u = -\frac{j_A}{D_A} + \frac{n_A \mu [A]}{L} \quad (4.15)$$

$$du = \frac{n_A \mu}{L} d[A] \quad (4.16)$$

$$\int \frac{L}{u n_A \mu} du = \int dz \quad (4.17)$$

One gets:

$$\frac{\ln(u)L}{n_A \mu} + C = \int dz \quad (4.18)$$

'u' in Equation 4.18 is substituted into Equation 4.15 and integrated from $[A]_{out}$ to $[A]_{in}$ and from L to 0.

$$\frac{\ln\left(\frac{-\frac{j_A}{D_A} + \frac{n_A \mu [A]}{L}}{n_A \mu}\right) L}{n_A \mu} \Bigg|_{[A]_{in}}^{[A]_{out}} = z \Big|_0^L \quad (4.19)$$

$$-n_A \mu = \ln\left(\frac{-\frac{j_A}{D_A} + \frac{n_A \mu [A]_{in}}{L}}{-\frac{j_A}{D_A} + \frac{n_A \mu [A]_{out}}{L}}\right) \quad (4.20)$$

$$\exp(-n_A \mu) = \frac{-\frac{j_A}{D_A} + \frac{n_A \mu [A]_{in}}{L}}{-\frac{j_A}{D_A} + \frac{n_A \mu [A]_{out}}{L}} \quad (4.21)$$

$$\exp(-n_A\mu) \frac{-j_A}{D_A} + \exp(-n_A\mu) \frac{n_A\mu[A_{out}]}{L} = \frac{-j_A}{D_A} + \frac{n_A\mu[A_{in}]}{L} \quad (4.22)$$

$$\frac{j_A}{D_A} (1 - \exp(-n_A\mu)) = \frac{n_A\mu[A_{in}]}{L} - \exp(-n_A\mu) \frac{n_A\mu[A_{out}]}{L} \quad (4.23)$$

$$\frac{j_A}{D_A} = \frac{\frac{n_A\mu[A_{in}]}{L} - \exp(-n_A\mu) \frac{n_A\mu[A_{out}]}{L}}{1 - \exp(-n_A\mu)} \quad (4.24)$$

$$\text{Let } P_A = \frac{D_A}{L} \quad (4.25)$$

P_A is the permeability of the ion through the membrane which is expressed as m/s.

$$j_A = \frac{n_A P_A ([A_{in}] - \exp(-n_A\mu)[A_{out}])}{1 - \exp(-n_A\mu)} \quad (4.26)$$

The electric current density (J_A) is related to the flux by, where q_A is the charge of the ion :

$$J_A = j_A q_A \quad (4.27)$$

Equation 4.26 is then equated with Equation 4.27 and The electric current density (J_A) is related to the flux by where q_A is the charge of the ion:

$$J_A = \frac{q_A n_A P_A ([A_{in}] - \exp(-n_A\mu)[A_{out}])}{1 - \exp(-n_A\mu)} \quad (4.28)$$

Assuming there is zero Na^+ ions in trans chamber, ($[\text{Na}^+]_{out} = 0$), its electric current density is:

$$J_{\text{Na}^+} = \frac{P_{\text{Na}^+} [\text{Na}^+]_{in}}{1 - \exp(-\mu)} \quad (4.29)$$

And for K^+ , assuming no K^+ ions in the cis chamber ($\text{K}^+_{in} = 0$),

$$J_{\text{K}^+} = \frac{-P_{\text{K}^+} \exp(-\mu) [\text{K}^+]_{out}}{1 - \exp(-\mu)} \quad (4.30)$$

The net current density is 0 at E_{rev} .

$$J_{\text{K}^+} + J_{\text{Na}^+} = 0 \quad (4.31)$$

Substituting Equation 4.29 and Equation 4.30 into Equation 4.31, the relative permeability between Na^+ and K^+ is shown as following:

$$\frac{P_{\text{Na}^+}}{P_{\text{K}^+}} = \frac{[\text{Na}^+]_{in}}{[\text{K}^+]_{in}} \exp\left(-\frac{FE_{rev}}{RT}\right) \quad (4.32)$$

The relative permeability between Na^+ and Ca^{2+} can be determined when assuming $\text{Ca}^{2+}_{in} = 0$ for Equation 4.26.

$$J_{\text{Ca}^{2+}} = \frac{-4P_{\text{Ca}^{2+}} \exp(-2\mu) [\text{Ca}^{2+}]_{out}}{1 - \exp(-2\mu)} \quad (4.33)$$

Assuming the total density of Na^+ and Ca^{2+} currents to be 0, Equation 4.29 and Equation 4.33 can be used to obtain:

$$\frac{-4P_{\text{Ca}^{2+}} \exp(-2\mu) [\text{Ca}^{2+}]_{out}}{1 - \exp(-2\mu)} + \frac{P_{\text{Na}^+} [\text{Na}^+]_{in}}{1 - \exp(-\mu)} = 0 \quad (4.34)$$

Rearrange formula to be $\frac{P_{\text{Na}^+}}{P_{\text{Ca}^{2+}}}$ and multiply the numerator and denominator by $(1 + \exp(-\mu))$,

$$\frac{P_{\text{Na}^+}}{P_{\text{Ca}^{2+}}} = \frac{4(1 - \exp(-\mu)) [\text{Ca}^{2+}]_{out} * (1 + \exp(-\mu))}{[\text{Na}^+]_{in} (1 - \exp(-2\mu)) * \exp(2\mu) * (1 + \exp(-\mu))} \quad (4.35)$$

The final equation which was expressed in Fatt and Ginsborn(1958) would be:

$$\frac{P_{\text{Na}^+}}{P_{\text{Ca}^{2+}}} = \frac{4[\text{Ca}^{2+}]_{out}}{[\text{Na}^+]_{in} \exp\left(\frac{FE_{rev}}{RT}\right) \left(1 + \exp\left(\frac{FE_{rev}}{RT}\right)\right)} \quad (4.36)$$

Therefore, by measuring the reversal potential under known buffer conditions, one can calculate the relative permeability of Na^+/K^+ and $\text{Na}^+/\text{Ca}^{2+}$ using Equation 4.32 and Equation 4.36, respectively.

4.2 Results and discussion

4.2.1 General set-up of the Bilayer workstation to characterize NaChBac

4.2.1.1 Perfusion

To determine how much perfusion is required to fully replace the buffer in the trans chamber, SG was used to quantify the concentration of Na^+ (Figure 4.2). The old buffer is replaced by perfusing it with the new buffer at 15X of the original buffer volume. This number may vary as it depends on the flow rate, which in turn is determined by the height of the exchange buffer and the controlling of the valve. For all experiments in the rest of the chapter, buffer exchange was done with 20 ml (i.e. 20X of the original volume).

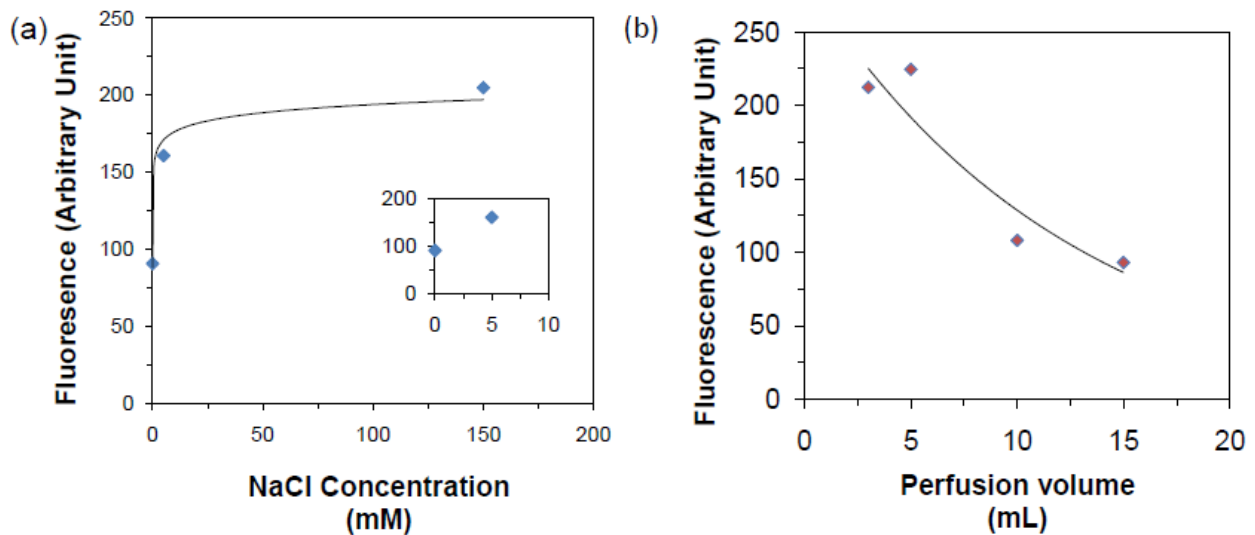


Figure 4.2 Optimization of perfusion condition for complete buffer exchange. (a) Fluorescence Intensity of 1 μM SG in 20mM Tris-Cl pH 7.4 buffer with 0, 5, and 150 mM NaCl using PTI fluorometer. (b) Fluorescence of 1 μM SG in the exchanged buffer when

150 mM NaCl is exchanged with distilled water. Only one single experiment was performed.

4.2.1.2 Voltage offset

The effect of liquid junction potential in the planar bilayer workstation was studied. Liquid junction potential is the potential difference which occurs when two different solutions are in contact with each other. As shown in the introduction of this chapter, the ion selectivity and ion permeability of a protein channel can be calculated by the reversal potential (E_{rev}) under appropriate conditions (see section 4.1.2). As a result, it is important to correctly determine the true membrane potential across the lipid bilayer housing the protein channel. The measured membrane potential (V_m) includes contributions from multiple sources:

$$V_m^{measured} = V_m^{true} + V_{offset}^{electrodes} + V_{offset}^{solutions} + V_{offset}^{amplifier} \quad (4.37)$$

$V_m^{measured}$ is the potential created or maintained by the function generator. V_m^{true} is the true potential difference experienced by the membrane. $V_{offset}^{electrodes}$ is the potential difference due to different concentration of Cl^- in the solution surrounding the Ag/AgCl electrodes. $V_{offset}^{solutions}$, also known as liquid junction potential, is the potential difference caused by different solutions interfacing with each other (Ng & Barry, 1995), and $V_{offset}^{amplifier}$, is the potential difference produced by the amplifier. This potential difference can be adjusted on the amplifier so that it cancels out the $V_{offset}^{electrodes}$ and $V_{offset}^{solutions}$. Correctly adjusting the voltage offset would ideally allow $V_m^{measured}$ to equal to V_m^{true} .

The BC-535 in our BLM workstation has an autozero function that allows us to cancel the $V_{offset}^{solutions}$ and $V_{offset}^{electrodes}$ with the $V_{offset}^{amplifier}$. The $V_{offset}^{amplifier}$ required for correcting both solution and electrode voltage offset is provided in Table 4.1.

Table 4.1. Offset voltages for different buffer conditions. Values were obtained from a single measurement.

Cis solution (mM)	Trans solution (mM)	$V_{offset}^{amplifier}$ (mV)
150 NaCl	50 NaCl	+4
	150 CaCl ₂	-4
	150 NaCl	-1
	150 KCl	+1

4.2.2 Conductance measurement of NaChBac

4.2.2.1 Conductance measurement of NaChBac at different NaCl concentrations

NaChBac's conductance changes depending on its environment (Ren et al., 2001; Studer et al., 2011). To determine if these changes are related to the concentration of NaCl, single channel conductance values were obtained by macroscopic current recordings in saline solutions with different [NaCl] (n=1) (Table 4.2). For 30/150 mM NaCl and 150/150 mM NaCl, the channel displays similar conductance values, 71.5 and 76.2 pS, respectively. However, under lower NaCl concentration, the

single channel conductance was 27.1 pS as determined by zero-voltage slope. This suggests that the conductance of NaChBac depends on the NaCl concentration. The E_{rev} under asymmetrical concentration (30 mM/150 mM NaCl) is -28.5 mV, whereas the calculated one is -40.6 mV. The measured E_{rev} under symmetrical concentration of NaCl is -9 mV and -5.7 mV for 150 mM and 30 mM, respectively (Table 4.2). The rectifying effect is only evident in 30 mM/30 mM NaCl (Figure 4.3) It cannot be told if it is an inward rectifying or outward rectifying effect here, as the orientation of the protein in the lipid bilayer is not known. The disagreement in the observed and calculated E_{rev} for the asymmetrical concentration suggests that there is Cl^- current, either due to membrane leakage or channel leakage, while the disagreement in the symmetrical concentration could possibly be due to its rectifying behavior. If the channel shows rectifying behaviour, it is difficult to correlate the zero-voltage slope without more data points near the zero-voltage since the rectification of the current makes the rate of change between the current and voltage in the I-V plot to be non constant.

Table 4.2. Conductance and E_{rev} of 6His-NaChBac under different NaCl concentrations.

One measurement was done for each condition.

Cis solution (mM)	Trans solution (mM)	Conductance (pS)	Observed E_{rev} (mV)	Theoretical E_{rev} (mV)
30	30	27.1	-5.7	0
30	150	71.5	-28.5	-40.6
150	150	76.2	-9.0	0

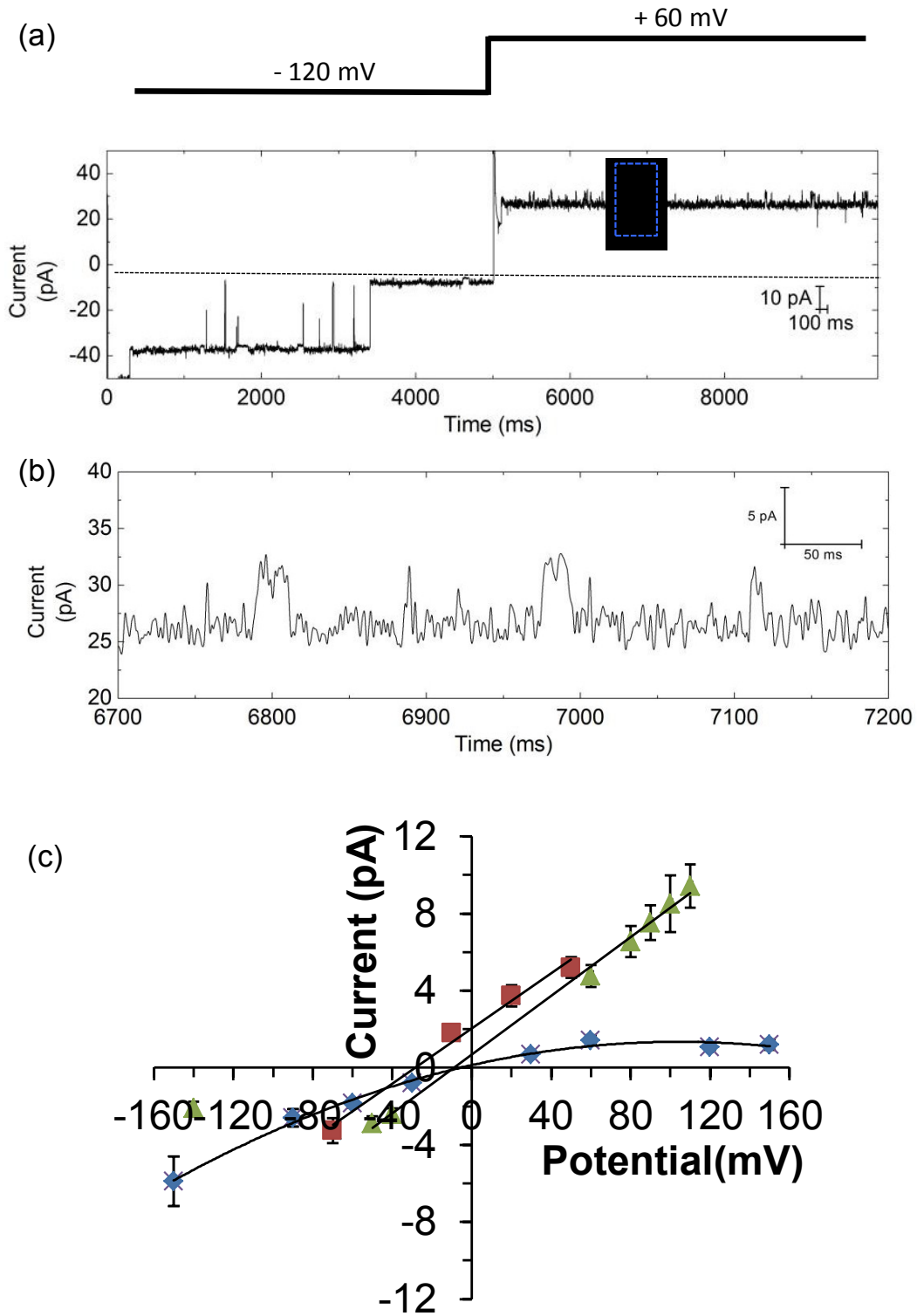


Figure 4.3. Macroscopic current recording of NaChBac under varied buffer conditions. (a) Top panel: example of voltage step (5 s at -120 mV followed by 5 s at +60 mV) that is used for the recording of (a) and (b). Bottom panel: the current trace under 150/150 mM NaCl. At -120 mV, the channels deactivate at around 3.7s and at +60 mV, the channels activate almost instantly. (b) A zoom of the dotted blue box from (a) showing opening events in individual channels. (c) The single channel I-V plot obtained from macroscopic current recording. Buffer conditions are as below: 30/30 mM NaCl (blue dots); 30/150 mM NaCl (red squares); and 150/150 mM NaCl (green triangles). Unitary channel conductance is summarized in Table 4.2. This was found using peak currents at various step potentials (mean \pm S.E.M., n = 40–100 events).

4.2.2.2 Selective blocking of channel activity using lidocaine N-ethyl bromide

One disadvantage of using the BLM approach is that membrane proteins may be incorporated into the membrane in either orientation. Some membrane proteins are reported to get inserted into lipid bilayer at a preferred orientation (Cough-Cardel, Hsueh, Wilkens, & Movileanu, 2016; Sumino, Sumikama, Iwamoto, Dewa, & Oiki, 2013), while most proteins are orientated in a random manner. The orientation of the voltage-gated ion channel will prevent proper data interpretation when it displays a rectifying or when studying the activation half voltage.

To solve this problem, lidocaine N-ethyl bromide, which is an intracellular blocker of NaChBac (S. Lee, Goodchild, & Ahern, 2012), can be added to block the activity of NaChBac. Lidocaine N-ethyl bromide was used over lidocaine as a blocker since

lidocaine N-ethyl bromide is membrane impermeable (Laffon Marc et al., 2002). Figure 4.4 shows the effect of lidocaine N-ethyl bromide on the NaChBac current. In this experiment, NaChBac protein was first incorporated into the lipid bilayer and two conducting levels were observed in the traces (Figure 4.4c). This suggests that the NaChBac has two protein channels opening at the same time, or it could also suggest that NaChBac has subconductance levels which will be discussed further in Section 4.2.2.3 where experiments performed in this thesis show that NaChBac has 3 subconducting levels. A voltage protocol as shown in Figure 4.4b was applied. Specifically, the holding potential was first set to -120 mV for 0.5 s before switching to +60 mV for 10 s. The voltage step is repeated 40 times. The capacitance current was canceled as explained in the Section 2.2.6.3.

Using the same inactivated trace for all experimental variables (i.e. no drug, adding drug, and washout) caused a baseline drift with respect to the current ensemble averages. To reduce the drift in the ensemble averages, 25 current traces were selected and averaged from each of the four ensemble averages with the inactivated currents deleted from each of the traces (H. K. Lee & Elmslie, 1999).

Another way to cancel capacitance current subtraction is to use currents from either a protein-free planar membrane or from a NaChBac incorporated membrane whose currents are blocked by a drug. This “dummy membrane” could be used to cancel out the capacitance current. According to Equation 4.11, the capacitance current is related to the membrane capacitance and its resistance and so if either value is

different to the membrane studied, the capacitive current may not be canceled completely.

Alternatively, capacitive currents can be cancelled using the P/N leak subtraction method (F Bezanilla & Armstrong, 1977). This method assumes the voltage applied is linearly proportional to the leak current. As long as the voltage difference between the control and experimental traces is the same, the current leak difference from the leak in the between each trace should also be the same. In this method, a control voltage pulse $1/N$ th of the test pulse voltage and is performed N times in the voltage range where the currents due to ion permeation would not be found. This creates current traces which includes only the capacitance and leak currents. The current trace amplitudes are added to form the control current which can be used to subtract out the leak and capacitance current. This is better than using the cancelling the capacitance using a “dummy membrane” since the membrane used to cancel the currents and the membrane used in the NaChBac experiments would be the same.

When lidocaine N-ethyl bromide (final concentration 4 mM) is added to the cis-side, the average peak current was reduced to baseline current (Figure 4.5b). Lidocaine N-ethyl bromide was also added to the trans side to block proteins that have their intracellular side facing the trans side and the cis side was perfused with buffer to washout the drug from the chamber. The ensemble average current for the drug washout and control was observed to have similar amplitude that suggest that the channels were oriented in the same direction. By adding the blocker to the cis chamber, the activity of NaChBac whose intracellular side is facing the cis chamber is suppressed.

Therefore, the protein channel experiences voltages with respect to its intracellular side. This means it experiences a voltage of opposite polarity when comparing with conventional voltage references which has the voltage with respect to the extracellular side. Said otherwise, when setting the holding potential to +60 mV and -120 mV, NaChBac whose intracellular side is facing the trans chamber will experience -60mV and +120 mV voltage). This would mean that the ion channel closing at +60 mV holding potential would be due to its deactivation as opposed to it being due to its inactivation.

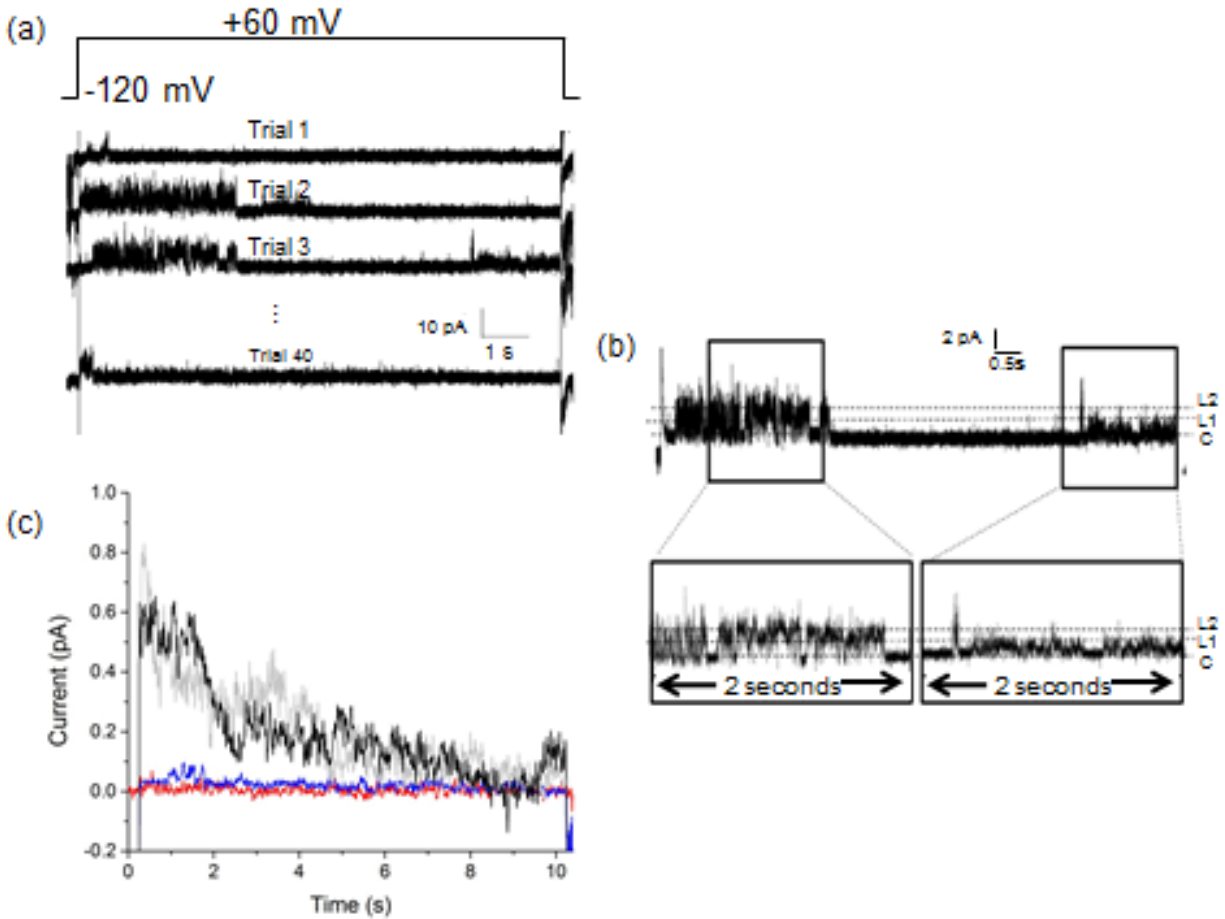


Figure 4.4. Inhibition of NaChBac by lidocaine N-ethyl bromide. (a) Top panel: voltage protocol used in this experiment. Bottom panel: 4 out of the 40 current traces from NaChBac channel recording before any addition of drug (4 mM lidocaine N-ethyl bromide). (b) Zoom-in of the third current trace from (a) which shows two conducting levels (L1 and L2). (c) Average current trace. Black: before any drug addition (i.e. control), red: after the addition of drug in the cis chamber, blue: after the addition of drug in cis and trans chamber, grey: after removal of drug from the cis chamber. Each current trace is the average of 40 recordings.

4.2.2.3 Conductance of NaChBac by single channel recording

As shown in previous section, a single fusion event of NaChBac-containing vesicles to the lipid bilayer introduced multiple copies of NaChBac protein and led to the observation of ensemble average currents. In order to obtain single channel activity, the protein to lipid ratio of the proteoliposome sample was subjected to optimization. Out of the protein to lipid ratios (wt/wt) used (i.e. 1:1000, 1:2000, and 1:3000), 1:3000 result in single channel insertion in the lipid bilayer.

Interestingly, more than one conducting states were observed when measuring the NaChBac conductance at single molecule level (Figure 4.5). Although some transitions among these three states are observed, for example transition from L3 to L2 at 3718 s (Figure 4.5d), majority of the opening events happens directly from a close state. That is, transition from a lower conducting state is not necessary. In other words, the opening of the channels is voltage dependent, and their destination states are random. The three sub-conducting states have the following values (Figure 4.5 and Figure 4.6): (1) Level 1 (L1) 26.4 ± 5.6 pS (mean \pm SEM, n=4), (2) Level 2 (L2) 92.8 ± 18.0 pS (n=3), and (3) Level 3 (L3): $268.5\text{pS} \pm 45.2$ (n=2). The value of L2 is similar to the conductance found in previous BLM studies (106 and 120 pS respectively (Saha et al., 2015; Studer et al., 2011)). L1 has value similar to that found in patch-clamp studies of NaChBac (12 pS (Ren et al., 2001)). However, L3, which is the highest conducting sub-state, has not been reported yet. The sharp transition from the closed state to L2 or L3 indicates they are sub-states of a protein but not the overall recording of multiple proteins. Subconducting states have been found in other proteins when studied by BLM.

For example Tom40, a mitochondrial outer membrane protein, was shown to exhibit 4 sub-states in BLM (Kuszak et al., 2015).

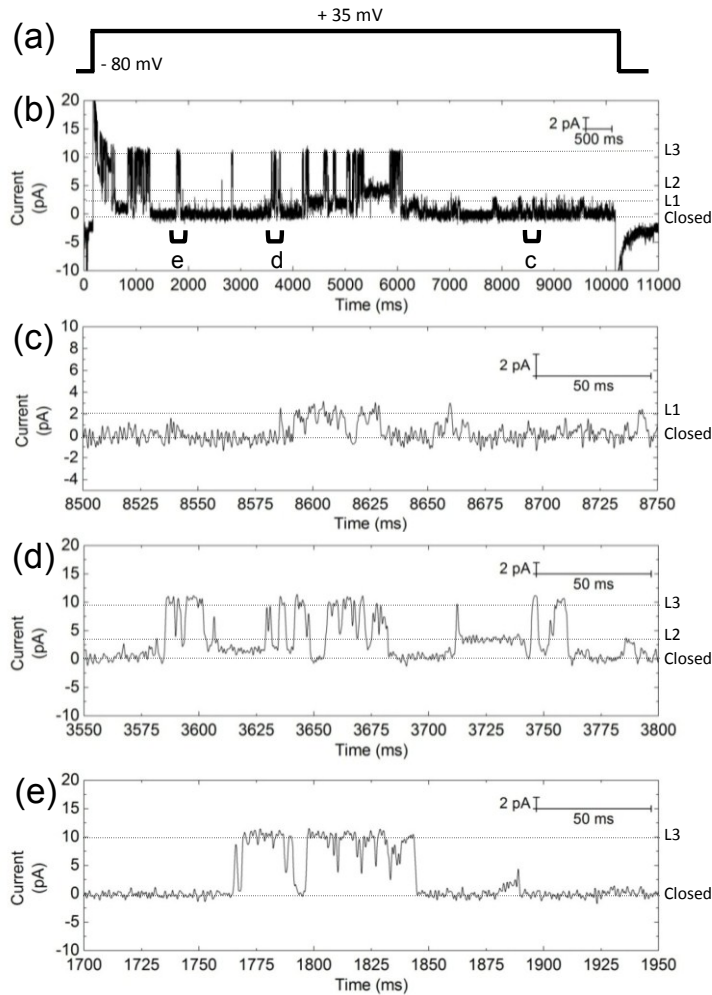


Figure 4.5. Single channel current recording of NaChBac. (a) Voltage protocol used for the measurement. The channel was undergone a voltage protocol of -80 mV for 0.2 s, followed by a step voltage at +35 mV for 10 s before the voltage is set back to -80 mV for 0.8 s. (b) A representative trace of the recording. Three conducting levels are observed. (c-e) Zoom-in image of each of the three conducting sub-states. The

experiment was repeated three times and the conductance were summarized in Table 3.3.

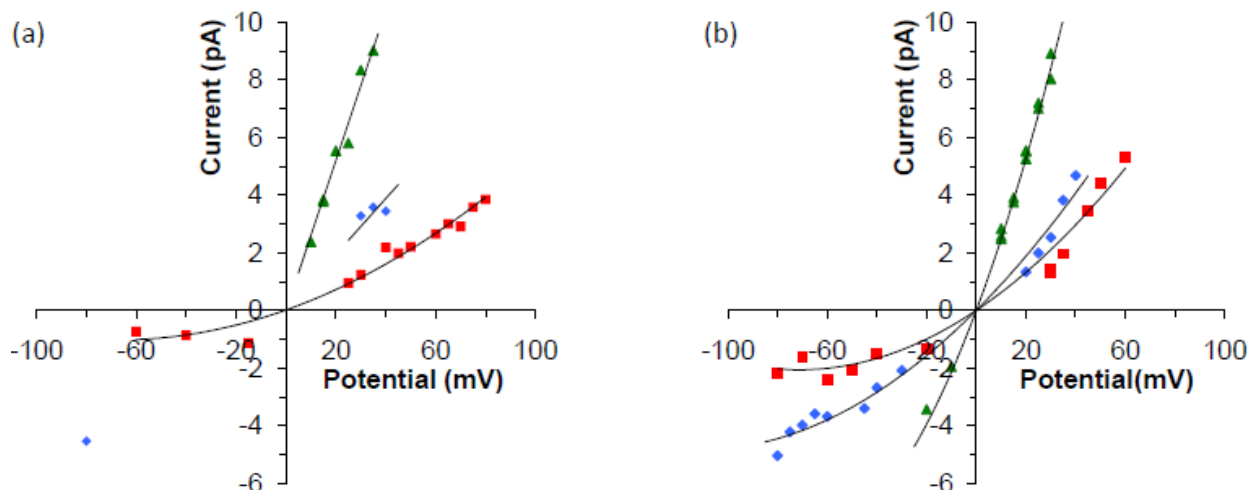


Figure 4.6. Single channel recordings with holding potentials from +80 to -80 mV in 5 mV increments. No data point displayed means no current events were found in that particular holding potential. (a) I-V plot in the absence of lidocaine N-ethyl bromide. While L1 (red square) opened in both positive and negative holding potentials, L3 (green triangle) and L2 (blue diamond) open less at lower potentials. (b) I-V plot of the same NaChBac in (a) in the presence of 4 mM lidocaine N-ethyl bromide in the cis chamber. The presence of the inhibitor increases the observation of channel opening to L2 and 3 states, particularly at negative holding potential.

To study the orientation of the protein, lidocaine N-ethyl bromide was added to the trans side of the bilayer (Figure 4.6). Channel activities, as well as the three-level conducting, remains observed. This suggests in this specific experiment, the intracellular side of NaChBac is located in the cis side of the bilayer. The protein is

inserted in an orientation that positive holding potential corresponds to a depolarizing effect to the protein. However, adding the inhibitor into the extracellular side has increased the observation of channel opening in the L1 and L2 states (Figure 4.6). The experiment was repeated twice and the results were summarized in Table 4.3 .

Table 4.3. The conductance of NaChBac in pS as obtained from single channel recording with 150 mM NaCl in both cis and trans chamber. Drug was added so there would be 4 mM of lidocaine n-ethyl bromide in the trans chamber. NA means that no current peak was found and ND means that the experiment did not take place.

	Lipid to protein ratio 3000:1					
	Exp 1		Exp 2		Exp 3	
	No Drug	Drug	No drug	Drug	No Drug	Drug
State 1	268.5	265.1	178.2	NA	ND	155.6
State 2	70.8	69.0	137.0	69.5	ND	94.3
State 3	31.0	35.0	42.3	32.8	ND	38.9

These results are in disagreement with previous studies that report single conducting states for NaChBac (Ren et al., 2001; Saha et al., 2015; Studer et al., 2011).

It is reported that formation of lipid channels in lipid bilayer may cause misinterpretation of protein properties. Lipid channels are formed when the temperature of the lipid bilayer is close to its melting temperature (T_m). The *E. coli* lipid used in my experiment has a T_m of $12.7 \pm 0.9^\circ\text{C}$ (Merino-Montero, Montero, & Hernández-Borrell,

2006), though the incorporation of membrane proteins may change the T_m of the lipid bilayer (Mosgaard & Heimburg, 2013). In addition, it has been reported that lipid channels display discrete conductance states ranging from 20 to 320 pS and with characteristics similar to protein channels such as single channel openings, multistep conductance bursts, and flickerings (Laub et al., 2012). Although lipid channels are not known to be voltage dependent on large membranes (~200 μm in diameter), lipid channels can also become voltage gated, when studying the channels on patch pipettes (Blicher & Heimburg, 2013). Lipid channel currents appear similar to protein channel currents, but their unpredictable nature causes their conductance to be inconsistent and unstable between experiments (Mosgaard & Heimburg, 2013). Given that (1) all BLM experiments in this thesis were performed at room temperature, (2) the observation of three sub-states can be repeated and (3) the current can be affected by lidocaine N-ethyl bromide (Figure 4.4b and Figure 4.6), it is unlikely that the subject in the single channel characterization is lipid channel.

The abnormal conducting behavior could result from contaminant proteins. Purifying membrane proteins is known to be difficult. There are many studies that found contaminant proteins in a “purified” sample even after multi-step purification (Psakis, Polaczek, & Essen, 2009; Wiseman et al., 2014). Common contaminant proteins found when purifying membrane protein in *E. coli* are AcrB and OmpF (Gutsmann, Heimburg, Keyser, Mahendran, & Winterhalter, 2015; Wiseman et al., 2014). AcrB is part of the efflux pump complex in *E. coli* that allows hydrophobic molecules such as antibiotics to be extruded from the periplasm to outside the outer membrane and is found to be

overexpressed when the cell is under growth pressure (Murakami, Nakashima, Yamashita, & Yamaguchi, 2002). OmpF, the other common contaminant, is a porin which is found to be related to *E.coli* resistance to drugs (Mahendran et al., 2010). To determine if the channel is OmpF, the experimenter can use micromolar amounts of enrofloxacin, an OmpF inhibitor, to determine if the currents are from the contaminant (Mahendran et al., 2010).

To check for contaminant proteins in our purified NaChBac sample, the protein was overloaded on a SDS-PAGE gel. Typically for SDS-PAGE gel detected with coomassie blue staining, 0.5 µg of purified protein sample will give a decent signal, while 10 µg will give a oversaturate signal. Accordingly, the SDS-PAGE was overloaded with 16 and 32 µg of purified NaChBac. Additional bands at 105 kDa and 50 kDa were clearly observed in addition to the NaChBac band (25 kDa) on the overloaded gel (Figure 4.7). It was previously thought that the faint bands at 50 kDa and 105 kDa are dimer and tetramer of NaChBac, respectively, as NaChBac is known to exist as a tetramer. The three major protein bands from the overloaded SDS-PAGE gel were collected and submitted for peptide fingerprinting mass spectrometry analysis to confirm their identity. When searching the MS spectra against the *E. coli* native protein library, it found that the 105 kDa band is AcrB and the 47 kDa is HemY. HemY is a peripheral membrane protein (Hansson & Hederstedt, 1994) and does not form any pore structure in the membrane for passage of ions. As mentioned in previous paragraph, AcrB is part of the *E. coli* efflux pump. It does have a transmembrane pore in its structure but it is a hydrophobic pore (with a diameter of 30 Å) which is found to be filled with phospholipids

(Murakami et al., 2002). Furthermore, a rough estimate of the percentage of the contaminant proteins was performed based on the band intensity. As shown in Table 4.4, at least 76% of the purified protein is NaChBac and AcrB and HemY only pose as minor contamination. However, the linear relationship between concentration and band intensity is only valid at low protein concentrations. As the NaChBac was overloaded, the real concentration of the 25 kDa band is beyond the linear region, thus the value obtained is an under-estimation. Therefore, it can be excluded that the observed Na^+ current is due to trace amount of contaminant proteins (i.e. AcrB and HemY) in the purified NaChBac sample.

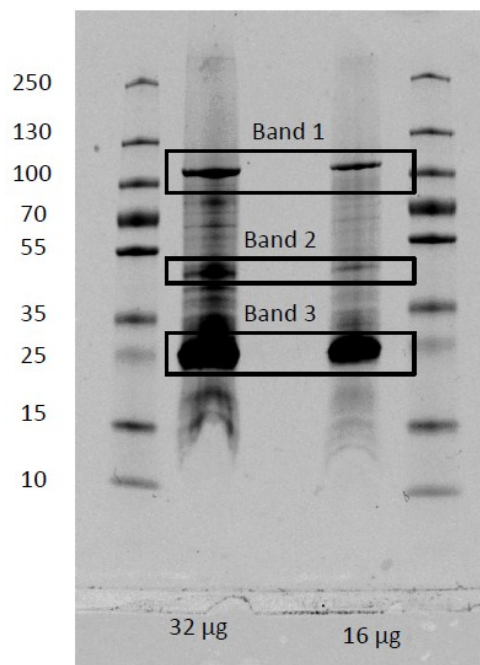


Figure 4.7. Overloading the SDS PAGE gel to look for contaminants.

Table 4.4. Components and relative concentrations in the purified NaChBac sample determined by SDS-PAGE and LC-MS.

Band #	Estimated MW (kDa)	Percentage 32 µg lane	Percentage 16 µg lane	Name	Theoretical MW (kDa)
1	105	15	9	AcrB	113.5
2	47	8	3	HemY	45.2
3	24	76	88	NaChBac	33.4

Other reasons for the sub-conductances found in my studies could be due to changes in buffer concentrations, temperature, type of lipid, or even protein-protein interactions (Fox, 1987; Gavillet et al., 2006; Schild, Ravindran, & Moczydlowski, 1991). Difference in conductance values suggests that NaChBac's conductance may depend on its surrounding environment (e.g. lipid bilayer environment).

4.2.2.4 Effect of N-terminal 6His-tag on the conductance of NaChBac

A 6His-tag was introduced into the protein sequence to facilitate protein purification. The purified NaChBac protein used for the characterization described in this thesis thus has a 6His-tag. The 6His-tag is relatively short, hence does not affect the

activity of the protein of interest (Bornhorst & Falke, 2000). To verify this, the conductance of the 6His-tagged and the tag-cleaved NaChBac were determined by macroscopic current recording. Cleaved and uncleaved NaChBac have similar conductance of 76 pS (Figure 4.8). However, further experiments are required to determine if the 6His-tag affects other properties such as activation and deactivation of the protein. The baseline for 6His-tagged and the tag-cleaved NaChBac shown in Figure 4.8 (a and b) are different as the baseline depends on the number of inserted protein channels. The more channels inserted into the lipid bilayer, the higher the current baseline, as more channels are being open at the same time.

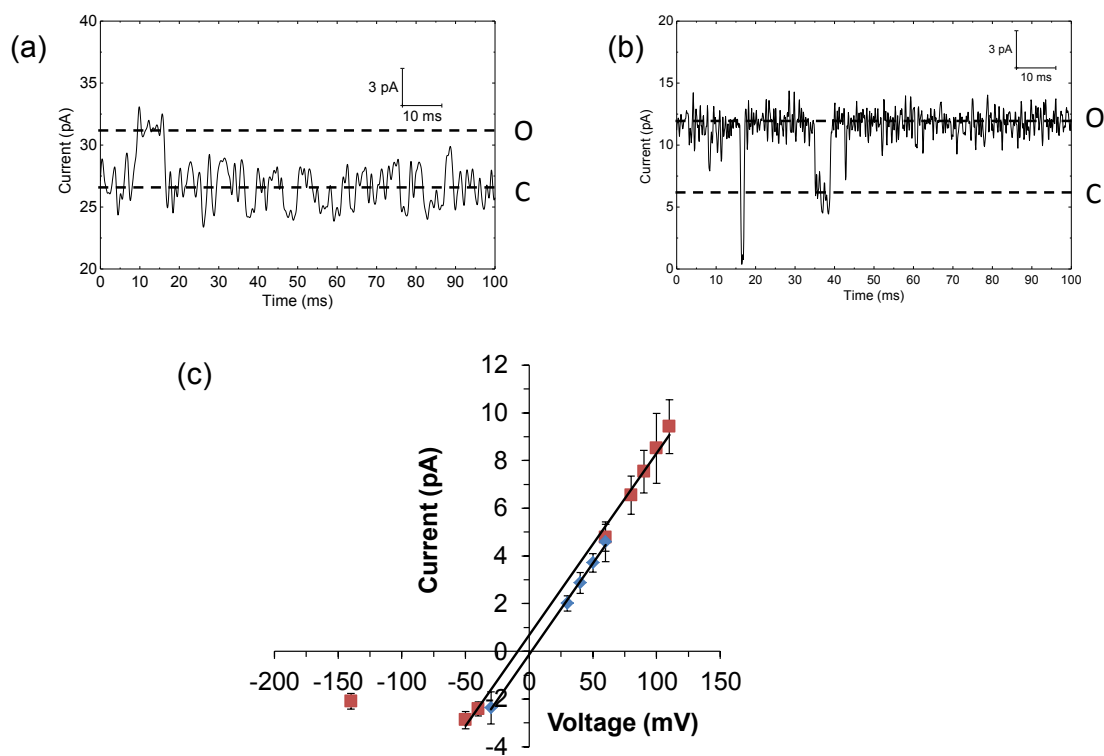


Figure 4.8. Conductance of tag-free NaChBac and 6His-NaChBac using peak single channel currents found by macroscopic current recording. (a) Exemplary current trace for tag-free NaChBac recorded at +60 mV. O denotes the transient opening of an individual channel, while C denotes the baseline. (b) Exemplary current trace for 6HIS-NaChBac at +60 mV. (c) I-V plot obtained from opening event analysis. The 6His-NaChBac (red square) and tag-free NaChBac (blue diamond) have similar conductance (76 pS and 77 pS, respectively). One measurement was performed for each protein.

4.2.3 Activation voltage of NaChBac by single channel recording

As NaChBac is a voltage-gated channel, I investigated its activation potential and gating behaviour using BLM and compared the results with those obtained from patch-clamp experiments (Ren et al., 2001). The experiment is done by applying a voltage on the channel long enough for the NaChBac to reach steady state and then a deactivation voltage is applied to the channel in which the channel undergoes conformational changes to block the ions moving through. Before the protein conformation change occurs, the current is recorded which should be representative to the channel open probability of when the activation potential was applied. Ideally this should be right after the protein is hyperpolarized, but due to not being able to completely cancel the capacitive currents, the currents used for calculation were 150 ms after the deactivation voltage was applied (Figure 4.9). I/I_{\max} , the normalized current, was plotted against the voltage and the curve fitted with 2-state Boltzmann function to describe NaChBac's activation gating behaviour. The Boltzmann function is the following:

$$y = A_2 + \frac{A_1 - A_2}{1 + \exp\left(\frac{V - V_{1/2}}{\frac{RT}{zF}}\right)} \quad (4.38)$$

Where A_1 is the maximum I/I_{\max} value, A_2 is the minimum I/I_{\max} value, V is the test voltage, $V_{1/2}$ is the half activation voltage, R is the gas constant with a value of 8.314 J/mol/K, T is the temperature with a value of 297.15 K, and z is the apparent gating charge.

The half activation voltage ($V_{1/2}$) and the apparent gating charge (z) are both found using the Boltzmann equation to help describe NaChBac's gating behaviour. $V_{1/2}$ describes the potential required for 50% open probability of the activatable channels. The $V_{1/2}$ value found was -28 mV (Figure 4.9 and Figure 4.5), which is similar to the -24 mV obtained by patch-clamp experiment (Ren et al., 2001). This suggests that the NaChBac examined in BLM and in patch-clamp have similar activation gating properties. The apparent activation gating charge, z , is described as the number of charges that move from one side of the membrane to the other during the gating process and is found to have a value of 15.8. Some of the charges may travel only partway through the membrane. Thus, the apparent activation gating charge found using the Boltzmann equation, does not necessarily equal to the total gating charge which can be found by limiting slope method or Q/N method. For example, if 3 charges only traveled through half the membrane distance, its apparent gating charge would be 1.5. In addition, since the two state Boltzmann equation (Equation 4.38) was fitted to Figure 4.9, the apparent activation gating charge is only accurate if NaChBac's kinetics can be explained in two states model in which the gating charges can move only between an open and closed

configuration (Francisco Bezanilla & Villalba-Galea, 2013). More than two states require the use of the limiting slope or Q/N method (Sigg & Bezanilla, 1997).

NaChBac's apparent activation gating charge was found to be 15.9 elementary charges in this work. This value is comparable to a patch-clamp study which reports NaChBac's total apparent gating charge to be 15.8 elementary charges when using the Q/N technique (Kuzmenkin, Bezanilla, & Correa, 2004). The Q/N technique tends to have a larger apparent gating charge since it includes the activation gating charge and two other charges: the lateral charge, which is the charge that move after activation, and the peripheral charge, which is the charge that moves independent from the activation process (Sigg & Bezanilla, 1997). Since the apparent activation gating charge is similar to when using the Q/N technique, this suggests that there are no lateral and peripheral charges. Both the activation $V_{1/2}$ and apparent activation gating charge z , are both comparable to patch clamp studies which suggest NaChBac's behaviour does not change in BLM or in patch-clamp.

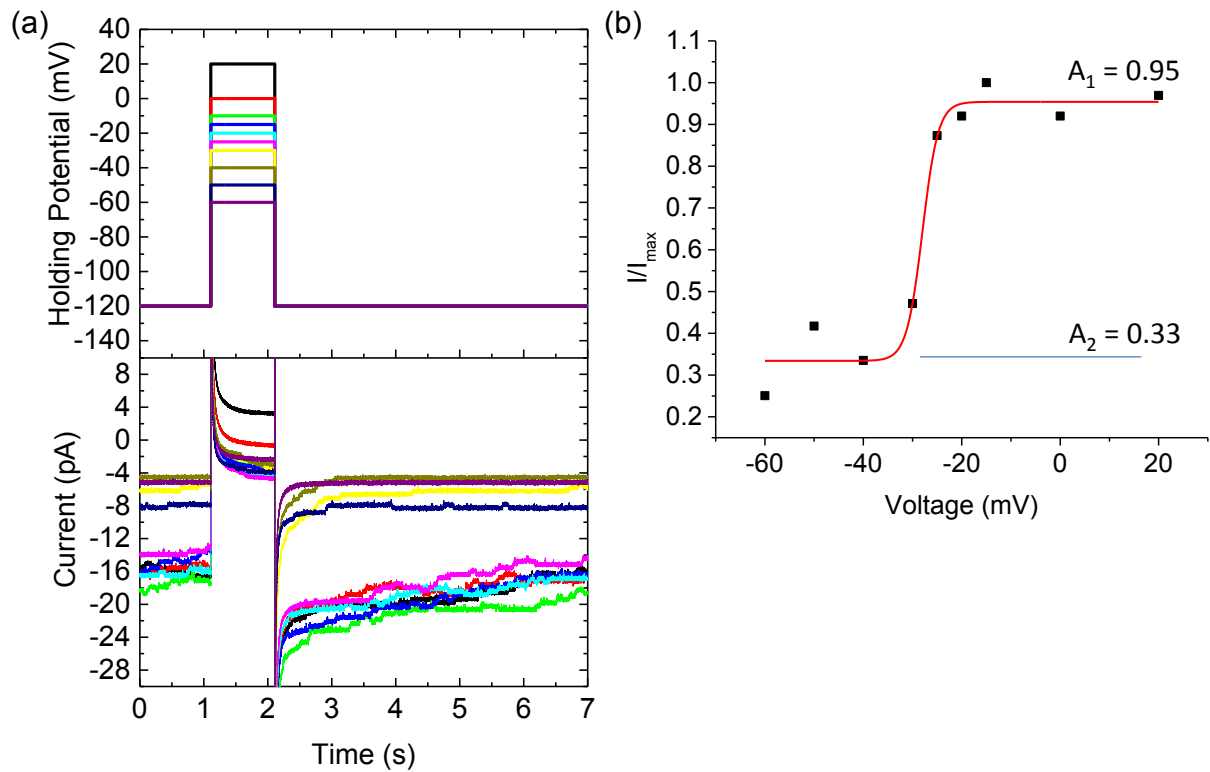


Figure 4.9. Activation curve of NaChBac. (a) Voltage protocol used to obtain the activation curve. Protein was first held at -120 mV before switching to various activation step voltages (+20 mV, 0 mV, -10 mV, -15 mV, -20 mV, -25 mV, -30 mV, -40 mV, -50 mV, and -60 mV as labelled by black, red, green, blue, turquoise, pink, yellow, dark yellow, dark blue, and dark purple, respectively). A deactivation voltage of -120 mV was applied subsequently. The current traces shown are the average current traces after the voltage protocol is applied. (b) The activation curve of NaChBac which was found by plotting the current at 150 ms after switching back to the holding voltage potential of -120 mV. The current was plotted using I-V curve and fitted using the 2-state Boltzmann function as discussed in the context.

4.2.4 Selectivity study of NaChBac with BLM

Previous studies using patch-clamp and NaChBac heterologously expressed in mammalian cells suggest that NaChBac is a Na^+ selective ion channel (Ren et al., 2001). In this section, the ion selectivity of NaChBac is investigated when purified NaChBac is reconstituted into a planar lipid bilayer. Two voltage protocols were used to determine the ion selectivity. In both cases, the cis side of the membrane is filled with a 150 mM NaCl buffer, while the trans side filled with a MCl buffer (M denotes the ion species to be tested) with the same concentration. In the first protocol, the NaChBac was first held at 30 mV for 5 s, followed by a step to the test potentials that ranges from +80 to -80 mV. The conducting currents at different voltage steps are recorded and the conductance and reversal potential evaluated from the I-V plot. This approach will be referred as bi-ionic condition protocol hereafter. In the second protocol, the E_{rev} under asymmetric solution was measured by voltage ramping in which the voltage is sweep at a speed of 100 mV/s from -100 mV to +100 mV. Hereafter this method is referred as voltage ramp. In both approaches, Na^+ ionic flux dominates the current when positive voltage is applied, while M^+ flux dominates the current when negative voltage is applied. Reversal potential, which is the membrane potential when there is no net charge movement (i.e. zero current), is then extracted from the plots. Relative permeability is calculated from the reversal potential and the salt concentrations using Equations 4.32 and Equation 4.36.

In the bi-ionic protocol, the currents were found using all point histograms. The reversal potential and thereby the relative permeability is determined from the x-intercept of the I-V curve. Remarkably, NaChBac shows conductance at far negative voltage for both Na^+/K^+ and $\text{Na}^+/\text{Ca}^{2+}$ conditions (Figure 4.10a-b). This would suggest that NaChBac is permeable to both K^+ and Ca^{2+} .

NaChBac displayed two transition sub-states at both positive and negative voltage under the Na^+/K^+ bi-ionic condition (Figure 4.10a). From the I-V curves two relative permeability values can be obtained with the lesser conducting state having a $P_{\text{Na}^+}/P_{\text{K}^+}$ value of 0.88 ± 0.03 ($n=2$, \pm SEM) and the larger conducting state having a $P_{\text{Na}^+}/P_{\text{K}^+}$ of 1.15 ± 0.01 ($n=3$, \pm SEM) (Table 4.5). This suggests that the NaChBac at the larger conducting state is less permeable to Na^+ than K^+ , whereas in the lesser conducting state it is more permeable to Na^+ than K^+ .

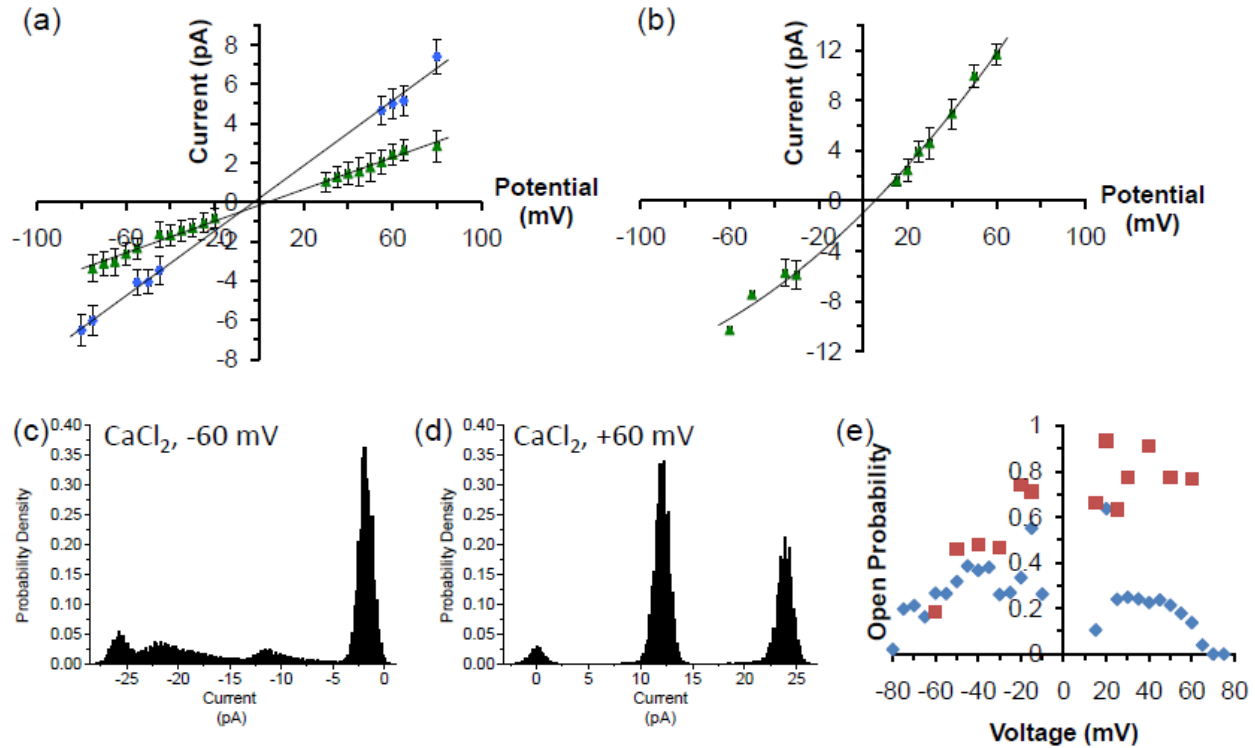


Figure 4.10. All point current histograms analysis for bi-ionic conditions for KCl and CaCl₂. I-V curve for NaChBac (a) 150/150 mM NaCl/KCl and (b) 150/150 mM NaCl/CaCl₂. Probability density function for CaCl₂ at (c) -60 mV and (d) +60 mV. (e) Open probability for KCl (blue diamond) and CaCl₂ (red square) bi-ionic conditions. Similar experiments were repeated three time and the result summarized in Table 4.5.

Similarly, the Na⁺/Ca²⁺ selectivity is found by the I-V plot obtained under Na⁺/Ca²⁺ bi-ionic conditions (Figure 4.10b and Table 4.5) with a value of $P_{Na^+}/P_{Ca^{2+}} = 1.43 \pm 0.20$ ($n=3$, \pm SEM). The result suggests that NaChBac is permeable to Ca²⁺, though Na⁺ ions are slightly more permeable than Ca²⁺ ions.

As the I-V plot only takes into account opening events, the opening probability of the channel was compared at different voltage to better understand the selectivity of NaChBac. For the $\text{Na}^+/\text{Ca}^{2+}$ bi-ionic condition, the opening probability observed at negative voltage was significantly lower than that at positive voltage (Figure 4.10c-e). It should be noted that there are two channels in this specific recording and the opening probability of an individual channel is calculated and plotted in Figure 4.10e. In this respect, NaChBac is less selective to Ca^{2+} than to Na^+ . The same opening probability analysis on the Na^+/K^+ condition does not provide any clear trend.

To further study the ion selectivity of NaChBac, the voltage ramp protocol was used to determine the reversal potential. In the voltage ramp protocol, the current is recorded when the voltage is held at -100 mV, then changed to 100 mV in 2 s and then held at -100 mV for another 0.5 s (Figure 4.11). 100 consecutive runs were recorded and the average was used to determine the E_{rev} . The voltage ramp experiments suggest that the $P_{\text{Na}^+}/P_{\text{K}^+}$ ranges from 0.86 to 1.35, and $P_{\text{Na}^+}/P_{\text{Ca}^{2+}} = 1.48 \pm 0.10$ ($n=3$, $\pm\text{SEM}$) (Table 4.5 and Table 4.6), consistent with the values obtained from the bi-ionic protocol. However, when examining individual traces, many traces were observed to have little or no channel opening events at negative voltage while channel opening events dramatically increase at positive voltage (Figure 4.11 a and c). Knowing that negative voltage drives K^+ or Ca^{2+} from the trans side to the cis side of the membrane and that positive voltage drives Na^+ from the cis side to the trans side, these traces suggest that there is Na^+ -mediated current, but no K^+ or Ca^{2+} -mediated current going through the channel.

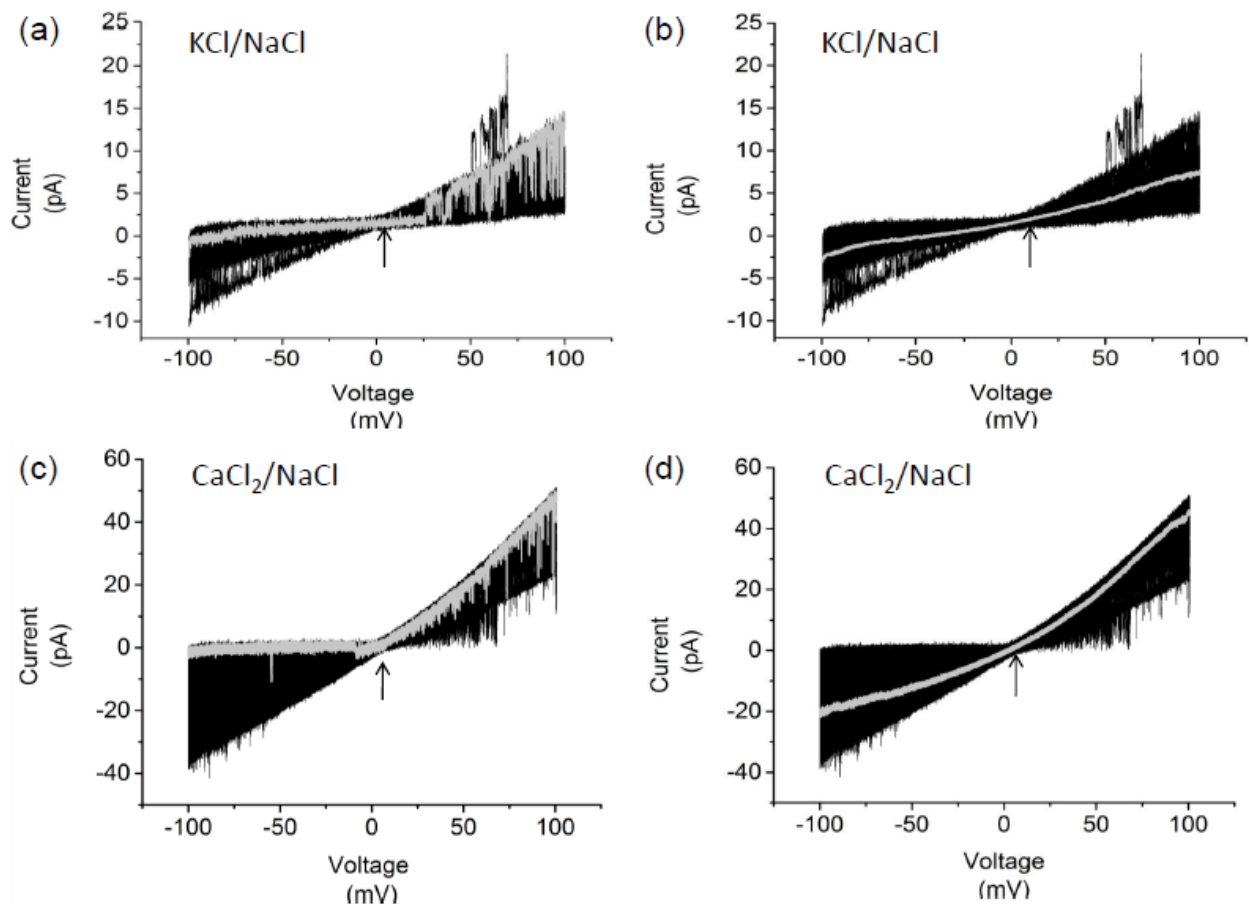


Figure 4.11. Voltage ramp under asymmetrical buffer condition. An overlap of 100 current traces when voltage ramps from -100 mV to 100 mV in 2 s are shown in dark lines. (a) Bi-ionic buffer with KCl in the trans side of the bilayer and NaCl in the cis side. A representative individual trace showing no K⁺ conductance is highlighted in grey. (b) Same data set as (a), with the average highlighted in grey. (c) Bi-ionic buffer with CaCl₂ in the trans side of the bilayer. A representative individual trace showing no K⁺ conductance is highlighted in grey. (d) Same data set as (c), with the average trace highlighted in grey. Arrow head indicated the reversal potential obtained from I-V plots.

Table 4.5. Na⁺/K⁺ selectivity of NaChBac. For Trial 2 and 3, two sub-states were found (denoted as a and b respectively) thus two E_{rev} and two relative permeability values can be derived.

Trial	E _{rev} (biionic condition)	P _{Na⁺} /P _{K⁺}	E _{rev} (voltage ramp)	P _{Na⁺} /P _{K⁺}
1	4.07	1.17	7.73	1.35
2a	-2.45	0.91	-2.60	0.90
2b	3.69	1.16		
3a	-4.30	0.85	-3.94	0.86
3b	3.27	1.14		

Table 4.6. Na⁺/Ca²⁺ selectivity of NaChBac

Trial	E _{rev} (biionic condition, mV)	P _{Na⁺} /P _{Ca²⁺}	E _{rev} (voltage ramp, mV)	P _{Na⁺} /P _{Ca²⁺}
1	7.67	1.26	7.48	1.28
2	1.57	1.82	3.30	1.65
3	8.46	1.20	4.57	1.82
Average	5.90	1.43	5.11	1.58

Bi-ionic condition with K^+ in the trans chamber and Na^+ in the cis chamber shows that K^+ has comparable permeability to Na^+ (Figure 4.10 and Table 4.5). Two subconductance levels were found, suggesting that K^+ has different permeabilities depending on the opening level. Bi-ionic condition with Ca^{2+} ions in the trans chamber shows that Ca^{2+} is less permeable than Na^+ ions. Patch-clamp studies on NaChBac have reported relative permeabilities for K^+ and Ca^{2+} (P_{Na^+}/P_{K^+} , $P_{Na^+}/P_{Ca^{2+}}$) to be 171 ± 16 (n=8) and 72 ± 10 (n=12), respectively (Ren et al., 2001). It was thus concluded that NaChBac is a Na^+ selective channel with selectivities comparable to classical eukaryotic Na_v channels. However as shown above, different selectivity behavior was observed for the reconstituted NaChBac in POPG/POPE lipid bilayer. The literature values are 2 orders of magnitudes greater than the values found in this thesis. This suggests that NaChBac behaviour changes when studying in BLM and in patch-clamp, most likely due to lipid environment.

4.2.5 Conclusions

NaChBac studied in BLM using artificial membranes displays different characteristics than in patch-clamp using mammalian cells. NaChBac incorporated in planar membranes was found here to open and close at three conducting levels. This was not observed previously in both BLM or in patch-clamp studies (Ren et al., 2001; Studer et al., 2011). While two of the three conducting levels were similar to reported values (Ren et al., 2001; Studer et al., 2011), the largest conducting level observed was not found in literature. In planar membranes, NaChBac was observed to be slightly

more permeable to Na^+ than Ca^{2+} , but depending on NaChBac's open state also depended whether K^+ is more or less permeable than Na^+ . In the Na^+ - K^+ bi-ionic experiment, NaChBac was observed to open and close at two conducting levels. The larger conducting level selected Na^+ less favorably than K^+ , and the lesser conducting level was observed to select Na^+ more favorably than K^+ . Patch-clamp studies suggest NaChBac in mammalian cells are more permeable towards Na^+ than both K^+ and Ca^{2+} and they were close to two orders of magnitude higher than the results found here. Nonetheless, NaChBac's activation half voltage (-28 mV) and apparent gating charge (15.8) were similar to some patch-clamp studies (Kuzmenkin et al., 2004; Ren et al., 2001). This suggests that its activation gating does not change when the channel is being studied in either artificial or mammalian membranes.

Chapter 5 Using Scattered Light Stopped-flow Spectroscopy to Study NaChBac

5.1 Introduction

During the course of this thesis work, different techniques were attempted, namely fluorescence flux assay and BLM, to characterize the prokaryotic voltage-gated sodium channel NaChBac as this protein is of interest to our project. However, ion channels are generally highly pursued in basic biological studies and pharmaceutical discovery due to their important biological functions. This chapter will discuss a new method for ion channel characterization and demonstrated its feasibility with NaChBac.

5.1.1 Advantages of using scattered light stopped-flow spectroscopy

As discussed in Chapter 3, fluorescence or radioactive flux assay is often used for ion channel characterization. Another method that may be used to study ion channels is using light scattering to follow the functionality and activity of ion channels. Previous studies have used stopped-flow spectroscopy to observe the swelling and shrinking of large unilamellar vesicles (LMVs) containing aquaporin in hypertonic or hypertonic solutions. Aquaporin is a class of membrane proteins that selectively transport water across the membrane, The scattered light stopped-flow flux assay has yet to be used to test the functionality of ion channels (Laganowsky et al., 2014). Light scattering method has the advantage that no indicator (neither fluorescent or radioactive) is required, and the use of stopped-flow allows data collection with high time resolution. This technique is especially useful compared to those who have a stopped-flow apparatus in their laboratory, but do not have the resources to study ion channels in

BLM, in patch-clamp, or for ion channels that don't have a functional indicator. It is also useful to pharmaceutical companies who are interested in ways to improve the speed of drug discovery.

5.1.2 Light scattering intensity changes of liposome

Given the size of the vesicle and the wavelength of the incident light, the scattering phenomenon during liposome swelling cannot be well described by the commonly used Rayleigh scattering theory. Instead, the Mie scattering that describes the light scattering of general spherical scattering solution without any particular bound on the particle size should be used. Rayleigh scattering comes into effect when the size of the particles is far smaller than the incident light ($mx \ll 1$, $m = n_{\text{sph}}/n_{\text{med}}$ is the ratio of the refractive index of the particle to that of the surrounding medium, and $x = (2\pi n_{\text{med}} a)/\lambda_0$ is the size parameter where a is the particle radius and λ_0 is the wavelength of the incident light). In our system, the radius of the vesicle is around 55 nm (Table 5.1), and the incident light used is 400 nm, giving an mx value of 1.2. The precise description between the scattering light intensity and the particle size in Mie scattering is complicated and there are some computer algorithms available online to calculate the numerical values (<http://www.philiplaven.com/mieplot.htm>). Furthermore, the liposome refractive index changes with respect to its volume change and this affects the light scattering intensity observed in stopped-flow spectroscopy (Latimer & Pyle, 1972). This relationship can be simplified and described using the following equation:

$$m(V) = 1 + (m_0 - 1)V_0/V \quad (5.1)$$

Where m_0 and V_0 are, respectively, the initial light scattering and volume of the liposome.

Including the refractive index changes to the Mie Scattering calculations, light scattering intensity decreases with liposome swelling and increases with liposome shrinkage. But this trend disappears when the 50 nm radius liposome shrinks to 1/5th its original volume (Figure 5.1), or liposome with larger radius (e.g. 400 nm) is used. Therefore, liposome prepared for the stopped-flow flux assay should not be much greater than 50 nm.

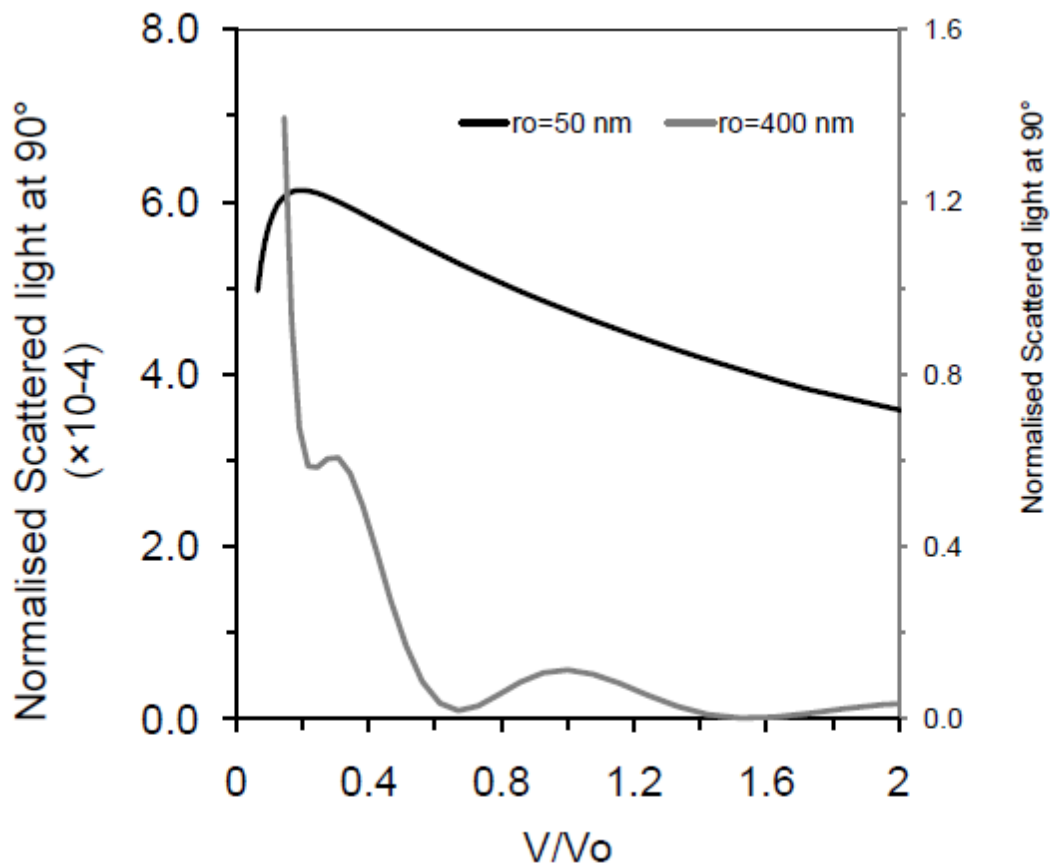


Figure 5.1. Normalized scattering light intensity is plotted with respect to the change in the volume for vesicles with radius of 50 and 400 nm at 400 nm incident light.

In this chapter, the functionality of NaChBac is measured by comparing the exponential decay of normalised light scattering intensity of NaChBac incorporated liposomes with control liposomes. This chapter will show that NaChBac vesicles are permeable to Na^+ , K^+ ions to the extent that it will cause the NaChBac vesicles to swell. The swelling is due to the protein as the ionic flux can be inhibited by a NaChBac blocker known as lidocaine.

5.2 Results and discussion

5.2.1 NaChBac vesicles functionality by scattered light stopped-flow spectroscopy

The vesicles are mixed with the mixing buffer in a clean mixing chamber and then the light scattering is detected at 90 degrees to the incident light (Figure 5.2a). The vesicles' light intensity increases when it swells and decreases when it shrinks (Figure 5.2b). When NaChBac vesicles enter a Na^+ hypertonic solution, the functioning NaChBac vesicles allow Na^+ to enter (Figure 5.2 and Figure 5.1c). When liposome without NaChBac (control) mixes with the buffer, no Na^+ is able to enter the vesicle and thus no scattering light change (Figure 5.2c). In one patch-clamp study (Ren et al., 2001), researchers showed that K^+ is close to being impermeable through NaChBac with Na^+ being 171 times more permeable than K^+ . However, in this light scattering

study, NaChBac vesicles are permeable to K^+ to the extent that the vesicles begin to swell (Figure 5.2d). This suggests that the selectivity filter of the NaChBac in this current study is different to that reported by Ren et al. (2001). This could be due to when incorporating membrane proteins to different membrane shows various functional activities (D'Avanzo et al., 2013; Laganowsky et al., 2014) or the experimental buffer conditions could be affecting NaChBac's selectivity filter.

Efforts have been made to increase the monodispersity of the vesicles by putting it through a Superdex 200 5/150 gel filtration column and collecting fractions of the vesicles. A gel filtration column separates samples by their hydrodynamic radius and hopefully the monodispersity will improve the reproducibility of the stopped-flow traces for the same sample. The size and polydispersity index (PDI) were measured before and after gel filtration using DLS (Malvern Zetasizer) and found that although the size of the vesicles from the fractions becomes progressively smaller, its PDI stays the same. To improve the PDI in future experiments, a size exclusion column with a more suitable fractioning range could be used to obtain sample with better PDI.

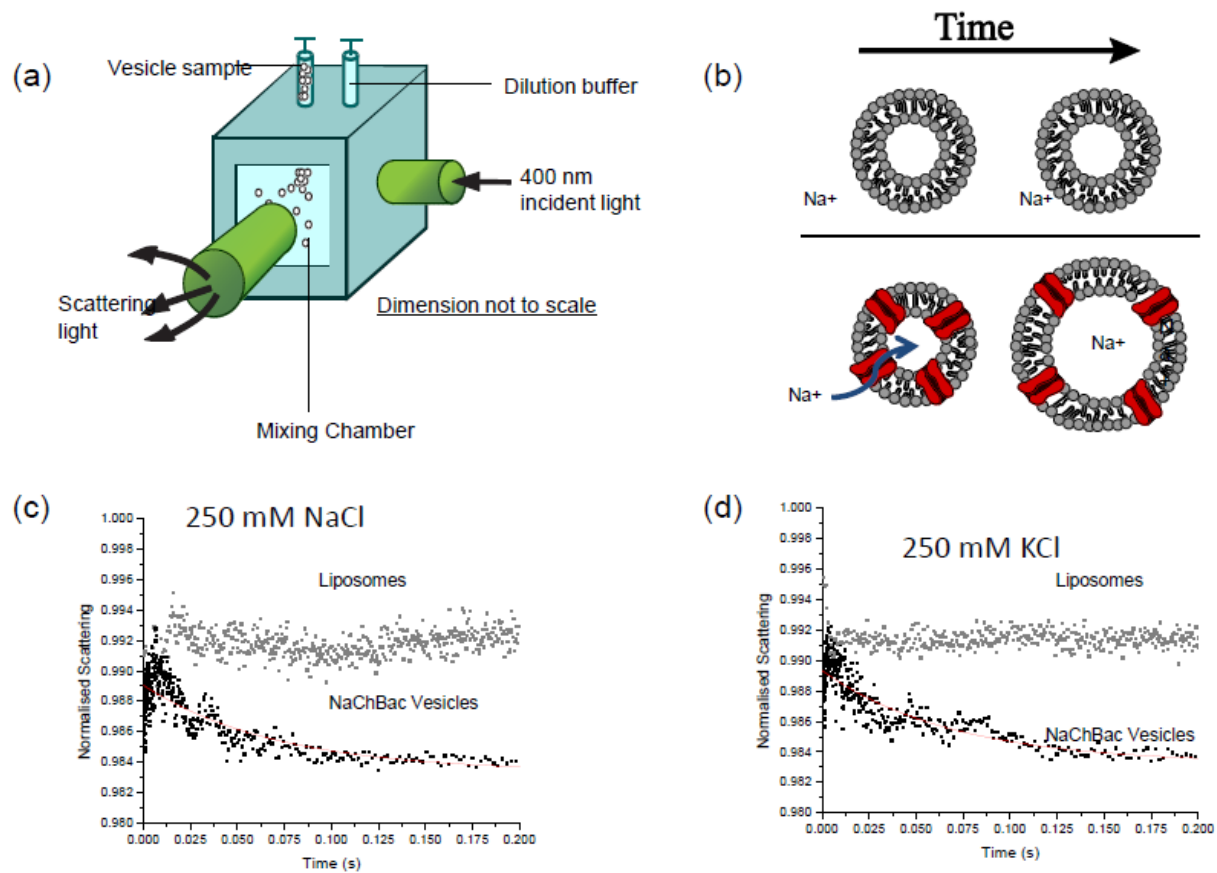


Figure 5.2. (a) A schematic diagram of the stopped-flow spectroscopy (b) Normalized scattering light intensities when NaChBac vesicles and control samples are mixed with 250 mM NaCl, 20 mM Tris-Cl, pH 7.2 (c) the NaChBac vesicles changing from isotonic to hypertonic solution (d) Normalized scattering light intensities when NaChBac vesicles and control samples are mixed with 250 mM KCl, 20 mM Tris-Cl, pH 7.2

Table 5.1. Size and polydispersity of liposome samples before and after Gel Filtration chromatography. The fraction highlighted in bold was used in the stopped-flow spectroscopy in the experiment discussed in Section 5.2.1.

Nth Fraction from Gel Filtration Chromatography	Control		NaChBac Vesicles	
	Z-average	PDI	Z-average	PDI
Before GFC	127.70	0.15	116.10	0.17
23	190.80	0.15	162.53	0.18
24	146.03	0.18	126.93	0.14
25	121.43	0.15	108.23	0.16
26	111.23	0.15	103.93	0.22

In another experiment, 100 nm diameter vesicles was used (Table 5.2) and the amount of NaChBac that was incorporated was increased to a 50:1 lipid to protein ratio. This experiment showed the magnitude and the k constant of the scattering intensity is greater than when vesicles with lipid to protein ratio of 100:1 was used (Figure 5.3). Possibly, by increasing the protein concentration incorporated into the liposomes, the membrane's Na⁺ permeability is increased. This would increase the rate the Na⁺ that will diffuse into the membrane and in turn, the liposomes would swell at a greater rate. The NaChBac vesicles tend to shrink from 20 ms to 50 ms, which indicates some

equilibrium pressures between the internal and external compartments of the NaChBac vesicles. To verify that the light scattering change is due to NaChBac's pore, NaChBac vesicles were incubated with lidocaine (final concentration: 1 mM) for 5 min and observed the light scattering when mixed with NaCl buffer (Figure 5.3). The light scattering behaviour was similar to that of the control, which suggests that the NaChBac vesicles were blocked entirely by lidocaine. This verifies that the light scattering observed is due to the ions entering through NaChBac.

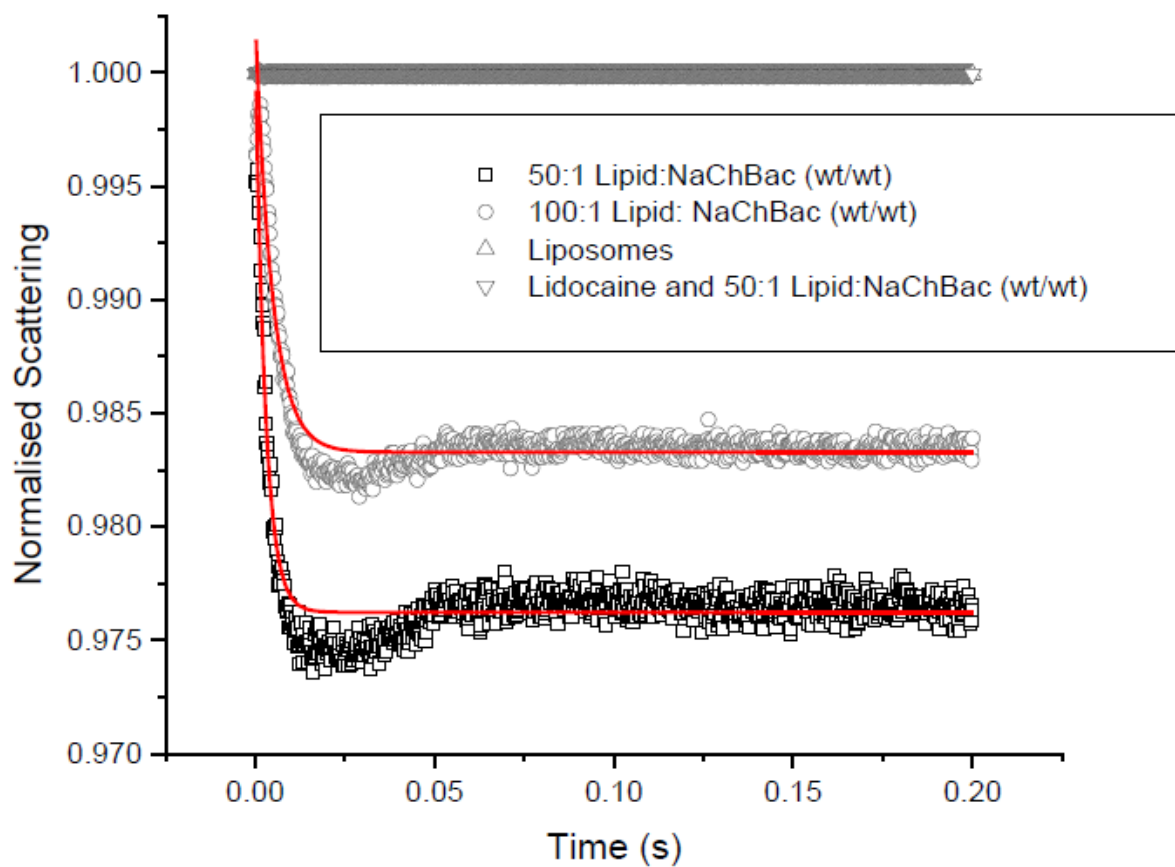


Figure 5.3. Normalized scattering light intensities when NaChBac vesicles and control samples are mixed with a hypertonic buffer.

Table 5.2. Diameter of the liposome vesicles used in the stopped-flow by using DLS instrument in the experiment found in Figure 5.2.

Lipid to Protein Ratio	Z-average \pm SD (n=3)	PDI \pm SD (n=3)
50:1	111.21 \pm 0.66	0.12 \pm 0.01
100: 1	111.43 \pm 0.13	0.10 \pm 0.01
Control	108.97 \pm 0.39	0.10 \pm 0.01

5.3 Conclusion

NaChBac vesicles introduced in a NaCl buffer solution will swell more than control liposomes. This is because the Na⁺ is permeable in NaChBac vesicles and allow water to get drawn into the membrane due to osmosis. The decrease in k constant found through

h stopped-flow spectroscopy, shows that 1 mM lidocaine can block NaChBac's functionality in liposomes. This suggests that this technique could potentially be used to find effective blockers for ion channels. For further research, stopped-flow spectroscopy is not limited to NaChBac and can be used to measure the functionality of other ion channels such as voltage-gated K⁺ channel from Aeropyrum pernix (KvAP). With further analysis on the light scattering intensity, it may be possible to investigate how the liposome swelling is related to ion flux. This information could be used to estimate the permeability of ions entering the liposomes which is important in further analyzing the kinetics of protein ion channels.

Chapter 6 Conclusions and Future Directions

NaChBac was purified and studied in artificial membranes. Its functionality was verified using Sodium Green encapsulated in liposomes. Furthermore, NaChBac's conductance and gating properties were found via BLM. NaChBac was also studied with stopped-flow spectroscopy by observing changes in the scattering light of the NaChBac vesicles corresponding to Na^+ influx.

The effectiveness of three encapsulation methods (freeze thaw method, direct hydration method, and sonication method) were tested. Each was tested by encapsulating Sodium Green dye (a Na^+ sensitive fluorophore) and observing fluorescence intensity. Freeze thaw method encapsulated the most dye while the sonication method encapsulated the least amount of dye. Direct hydration encapsulated an intermediate amount of dye. The freeze thaw method was therefore used to investigate NaChBac's functionality. NaChBac was tested by incorporation into liposomes into which Sodium Green had been encapsulated. Liposomes with membrane incorporated NaChBac had a higher fluorescence change in a NaCl buffer solution than liposomes with no NaChBac. This suggests that the NaChBac purified in this work is functional and the protein increases the liposomes permeability to Na^+ ions.

NaChBac was studied in BLM using artificial membranes. NaChBac incorporated in planar membranes were found to open and close at three conducting levels and was slightly more permeable to Na^+ than Ca^{2+} . In the Na^+ - K^+ bi-ionic experiment, NaChBac was observed to open and close at two conducting levels. The larger conducting level selected Na^+ less favorably than K^+ , and the lesser conducting level was observed to select Na^+ more favorably than K^+ ions. Patch-clamp studies

suggest NaChBac in mammalian cells are more permeable to Na^+ than they are to both K^+ and Ca^{2+} . NaChBac specificity in those experiments was found to be close to two orders of magnitude greater than the results found here. NaChBac's activation half voltage and apparent gating charge were comparable to some patch-clamp studies which suggests that its activation gating does not change when the channel is being studied in either artificial or mammalian membranes. Further research would involve comparing the inactivation gating of NaChBac in planar bilayers with NaChBac reported in patch clamp studies.

When studying NaChBac vesicles using stopped-flow spectroscopy, NaChBac vesicles light scattering intensity demonstrates an exponential decay as it gets introduced to a NaCl buffer solution. This suggests that NaChBac containing vesicles swell in NaCl buffer. No change in light scattering intensity was observed after performing the same experiment with NaChBac vesicles that were incubated with 1 mM lidocaine (a Na^+ channel blocker) for 10 min. This suggests that this technique could potentially be used to find effective blockers for any ion channel. Further research would involve using stopped-flow spectroscopy to measure the light scattering of other ion channels such KvAP and also to investigate ways to estimate the permeability of ions entering the liposomes which is important in further analyzing the kinetics of protein ion channels.

References

- Allen, T. M., Romans, A. Y., Kercret, H., & Segrest, J. P. (1980). Detergent removal during membrane reconstitution. *Biochimica et Biophysica Acta (BBA) - Biomembranes*, 601, 328–342. [http://doi.org/10.1016/0005-2736\(80\)90537-4](http://doi.org/10.1016/0005-2736(80)90537-4)
- Bezanilla, F., & Armstrong, C. M. (1977). Inactivation of the sodium channel. I. Sodium current experiments. *The Journal of General Physiology*, 70 (5), 549–566. <http://doi.org/10.1085/jgp.70.5.549>
- Bezanilla, F., & Villalba-Galea, C. A. (2013). The gating charge should not be estimated by fitting a two-state model to a Q-V curve. *The Journal of General Physiology*, 142(6), 575–578. <http://doi.org/10.1085/jgp.201311056>
- Blicher, A., & Heimbürg, T. (2013). Voltage-Gated Lipid Ion Channels. *PLoS ONE*, 8(6), e65707. Retrieved from <http://dx.doi.org/10.1371/journal.pone.0065707>
- Bornhorst, J. A., & Falke, J. J. (2000). [16] Purification of Proteins Using Polyhistidine Affinity Tags. *Methods in Enzymology*, 326, 245–254. Retrieved from <http://www.ncbi.nlm.nih.gov/pmc/articles/PMC2909483/>
- Catterall, W. A. (2001). A One-Domain Voltage-Gated Sodium Channel in Bacteria. *Science*, 294(5550), 2306–2308. Retrieved from <http://science.sciencemag.org/content/294/5550/2306.abstract>
- Chahine, M., Pilote, S., Pouliot, V., Takami, H., & Sato, C. (2004). Role of Arginine Residues on the S4 Segment of the *Bacillus halodurans* Na⁺ Channel in Voltage-sensing. *The Journal of Membrane Biology*, 201(1), 9–24. <http://doi.org/10.1007/s00232-004-0701-z>
- Charalambous, K., & Wallace, B. A. (2011). NaChBac: The Long Lost Sodium Channel Ancestor. *Biochemistry*, 50(32), 6742–6752. <http://doi.org/10.1021/bi200942y>
- Cleverley, D. Z., Geller, H. M., & Lenard, J. (1997). Characterization of cholesterol-free insect cells infectible by baculoviruses: effects of cholesterol on VSV fusion and infectivity and on cytotoxicity induced by influenza M2 protein. *Experimental Cell Research*, 233(2), 288–96. <http://doi.org/10.1006/excr.1997.3573>
- Colquhoun, D., & Hawkes, A. G. (1995). The Principles of the Stochastic Interpretation of Ion-Channel Mechanisms. In B. Sakmann & E. Neher (Eds.), *Single-Channel Recording* (pp. 397–482). Boston, MA, MA: Springer US. http://doi.org/10.1007/978-1-4419-1229-9_18
- Colquhoun, D., & Sigworth, F. J. (1995). Single-Channel Recording. In B. Sakmann & E. Neher (Eds.), (pp. 483–587). Boston, MA: Springer US. http://doi.org/10.1007/978-1-4419-1229-9_19
- Costa, A. P., Xu, X., & Burgess, D. J. (2014). Freeze-anneal-thaw cycling of unilamellar liposomes: Effect on encapsulation efficiency. *Pharmaceutical Research*, 31(1), 97–103. <http://doi.org/10.1007/s11095-013-1135-z>

- Couoh-Cardel, S., Hsueh, Y.-C., Wilkens, S., & Movileanu, L. (2016). Yeast V-ATPase Proteolipid Ring Acts as a Large-conductance Transmembrane Protein Pore. *Scientific Reports*, 6, 24774. Retrieved from <http://dx.doi.org/10.1038/srep24774>
- D'Avanzo, N., McCusker, E. C., Powl, A. M., Miles, A. J., Nichols, C. G., & Wallace, B. A. (2013). Differential Lipid Dependence of the Function of Bacterial Sodium Channels. *PLoS ONE*, 8(4). <http://doi.org/10.1371/journal.pone.0061216>
- Darszon, A. (1983). Strategies in the reassembly of membrane proteins into lipid bilayer systems and their functional assay. *Journal of Bioenergetics and Biomembranes*, 15(6), 321–334. <http://doi.org/10.1007/BF00751053>
- Eisenman, G., & Horn, R. (1983). Ionic selectivity revisited: The role of kinetic and equilibrium processes in ion permeation through channels. *The Journal of Membrane Biology*, 76(3), 197–225. <http://doi.org/10.1007/BF01870364>
- Epanand, R. F., Lehrer, R. I., Waring, A., Wang, W., Maget-Dana, R., Lelièvre, D., & Epanand, R. M. (2003). Direct comparison of membrane interactions of model peptides composed of only leu and lys residues. *Biopolymers - Peptide Science Section*, 71(1), 2–16. <http://doi.org/10.1002/bip.10372>
- Fatt, P., & Ginsborg, B. L. (1958). The ionic requirements for the production of action potentials in crustacean muscle fibres. *The Journal of Physiology*, 142(3), 516–543. <http://doi.org/10.1113/jphysiol.1958.sp006034>
- Fox, J. A. (1987). Ion channel subconductance states. *The Journal of Membrane Biology*, 97(1), 1–8. <http://doi.org/10.1007/BF01869609>
- Gavillet, B., Rougier, J.-S., Domenighetti, A. A., Behar, R., Boixel, C., Ruchat, P., ... Abriel, H. (2006). Cardiac Sodium Channel Nav1.5 Is Regulated by a Multiprotein Complex Composed of Syntrophins and Dystrophin. *Circulation Research*, 99(4), 407–414. <http://doi.org/10.1161/01.RES.0000237466.13252.5e>
- Goldman, D. E. (1943). POTENTIAL, IMPEDANCE, AND RECTIFICATION IN MEMBRANES. *The Journal of General Physiology*, 27(1), 37–60. <http://doi.org/10.1085/jgp.27.1.37>
- Gutsmann, T., Heimburg, T., Keyser, U., Mahendran, K. R., & Winterhalter, M. (2015). Protein reconstitution into freestanding planar lipid membranes for electrophysiological characterization. *Nat. Protocols*, 10(1), 188–198. Retrieved from <http://dx.doi.org/10.1038/nprot.2015.003>
- Hansson, M., & Hederstedt, L. (1994). Bacillus subtilis HemY is a peripheral membrane protein essential for protoheme IX synthesis which can oxidize coproporphyrinogen III and protoporphyrinogen IX. *Journal of Bacteriology*, 176(19), 5962–5970. Retrieved from <http://jb.asm.org/content/176/19/5962.abstract>
- Hodgkin, A. L., & Huxley, A. F. (1952a). A quantitative description of membrane current and its application to conduction and excitation in nerve. *The Journal of Physiology*, 117(4), 500–544. Retrieved from

<http://www.ncbi.nlm.nih.gov/pmc/articles/PMC1392413/>

- Hodgkin, A. L., & Huxley, A. F. (1952b). Currents carried by sodium and potassium ions through the membrane of the giant axon of Loligo. *The Journal of Physiology*, 116(4), 449–472. Retrieved from <http://www.ncbi.nlm.nih.gov/pmc/articles/PMC1392213/>
- Kelly, M. L., & Woodbury, D. J. (2003). *Planar Lipid Bilayers (BLMs) and Their Applications. Membrane Science and Technology* (Vol. 7). Elsevier. [http://doi.org/10.1016/S0927-5193\(03\)80049-9](http://doi.org/10.1016/S0927-5193(03)80049-9)
- Kido, H., Micic, M., Smith, D., Zoval, J., Norton, J., & Madou, M. (2007). A novel, compact disk-like centrifugal microfluidics system for cell lysis and sample homogenization. *Colloids and Surfaces B: Biointerfaces*, 58(1), 44–51. <http://doi.org/10.1016/j.colsurfb.2007.03.015>
- Kuszak, A. J., Jacobs, D., Gurnev, P. A., Shiota, T., Louis, J. M., Lithgow, T., ... Buchanan, S. K. (2015). Evidence of Distinct Channel Conformations and Substrate Binding Affinities for the Mitochondrial Outer Membrane Protein Translocase Pore Tom40. *Journal of Biological Chemistry*, 290 (43), 26204–26217. <http://doi.org/10.1074/jbc.M115.642173>
- Kuzmenkin, A., Bezanilla, F., & Correa, A. M. (2004). Gating of the Bacterial Sodium Channel, NaChBac: Voltage-dependent Charge Movement and Gating Currents. *The Journal of General Physiology*, 124(4), 349–356. <http://doi.org/10.1085/jgp.200409139>
- Laffon Marc, M. D., Jayr Christian, M. D., Barbry Pascal, P. D., Wang Ybing, M. D., Folkesson Hans G., P. D., Pittet Jean-Francois, M. D., ... Matthay Michael A., M. D. (2002). Lidocaine Induces a Reversible Decrease in Alveolar Epithelial Fluid Clearance in Rats. *Anesthesiology*, 96(2), 392–399. Retrieved from <http://dx.doi.org/>
- Laganowsky, A., Reading, E., Allison, T. M., Ulmschneider, M. B., Degiacomi, M. T., Baldwin, A. J., & Robinson, C. V. (2014). Membrane proteins bind lipids selectively to modulate their structure and function. *Nature*, 510(7503), 172–5. <http://doi.org/10.1038/nature13419>
- Latimer, P., & Pyle, B. E. (1972). Light Scattering at Various Angles. *Biophysical Journal*, 12(7), 764–773. [http://doi.org/10.1016/S0006-3495\(72\)86120-4](http://doi.org/10.1016/S0006-3495(72)86120-4)
- Laub, K. R., Witschas, K., Blicher, A., Madsen, S. B., Lückhoff, A., & Heimburg, T. (2012). Comparing ion conductance recordings of synthetic lipid bilayers with cell membranes containing TRP channels. *Biochimica et Biophysica Acta (BBA) - Biomembranes*, 1818(5), 1123–1134. <http://doi.org/10.1016/j.bbamem.2012.01.014>
- Lee, H. K., & Elmslie, K. S. (1999). Gating of Single N-type Calcium Channels Recorded from Bullfrog Sympathetic Neurons. *The Journal of General Physiology*, 113(1), 111–124.

- Lee, S., Goodchild, S. J., & Ahern, C. A. (2012). Local anesthetic inhibition of a bacterial sodium channel. *The Journal of General Physiology*, 139 (6), 507–516. <http://doi.org/10.1085/jgp.201210779>
- Maathuis, F. J. M., Taylor, A. R., Assmann, S. M., & Sanders, D. (1997). Seal-promoting solutions and pipette perfusion for patch clamping plant cells. *Plant Journal*, 11(4), 891–896. <http://doi.org/10.1046/j.1365-313X.1997.11040891.x>
- Mahendran, K. R., Hajjar, E., Mach, T., Lovelle, M., Kumar, A., Sousa, I., ... Ceccarelli, M. (2010). Molecular Basis of Enrofloxacin Translocation through OmpF, an Outer Membrane Channel of Escherichia coli - When Binding Does Not Imply Translocation. *The Journal of Physical Chemistry B*, 114(15), 5170–5179. <http://doi.org/10.1021/jp911485k>
- Marty, A., & Neher, E. (1995). Single-Channel Recording. In B. Sakmann & E. Neher (Eds.), (pp. 31–52). Boston, MA: Springer US. http://doi.org/10.1007/978-1-4419-1229-9_2
- Mayer, L. D., Hope, M. J., Cullis, P. R., & Janoff, A. S. (1985). Solute distributions and trapping efficiencies observed in freeze-thawed multilamellar vesicles. *Biochimica et Biophysica Acta (BBA) - Biomembranes*, 817(1), 193–196. [http://doi.org/10.1016/0005-2736\(85\)90084-7](http://doi.org/10.1016/0005-2736(85)90084-7)
- Merino-Montero, S., Montero, M. T., & Hernández-Borrell, J. (2006). Effects of lactose permease of Escherichia coli on the anisotropy and electrostatic surface potential of liposomes. *Biophysical Chemistry*, 119(1), 101–5. <http://doi.org/10.1016/j.bpc.2005.09.005>
- Mosgaard, L. D., & Heimburg, T. (2013). Lipid Ion Channels and the Role of Proteins. *Accounts of Chemical Research*, 46(12), 2966–2976. <http://doi.org/10.1021/ar4000604>
- Murakami, S., Nakashima, R., Yamashita, E., & Yamaguchi, A. (2002). Crystal structure of bacterial multidrug efflux transporter AcrB. *Nature*, 419(6907), 587–593. Retrieved from <http://dx.doi.org/10.1038/nature01050>
- Neuman, M. (1999). Biopotential Electrodes. In *The Biomedical Engineering Handbook, Second Edition. 2 Volume Set.* CRC Press. <http://doi.org/doi:10.1201/9781420049510.ch48>
- Ng, B., & Barry, P. H. (1995). The measurement of ionic conductivities and mobilities of certain less common organic ions needed for junction potential corrections in electrophysiology. *Journal of Neuroscience Methods*, 56(1), 37–41. [http://doi.org/10.1016/0165-0270\(94\)00087-W](http://doi.org/10.1016/0165-0270(94)00087-W)
- Nurani, G., Radford, M., Charalambous, K., O'Reilly, A. O., Cronin, N. B., Haque, S., & Wallace, B. a. (2008). Tetrameric bacterial sodium channels: characterization of structure, stability, and drug binding. *Biochemistry*, 47(31), 8114–21. <http://doi.org/10.1021/bi800645w>

- Ollivon, M., Lesieur, S., Grabielle-Madellmont, C., & Paternostre, M. (2000). Vesicle reconstitution from lipid–detergent mixed micelles. *Biochimica et Biophysica Acta (BBA) - Biomembranes*, 1508(1), 34–50. [http://doi.org/10.1016/S0304-4157\(00\)00006-X](http://doi.org/10.1016/S0304-4157(00)00006-X)
- Patti, J. T., & Montemagno, C. D. (2007). Fluorometric functional assay for ion channel proteins in lipid nanovesicle membranes. *Nanotechnology*, 18(32), 325103. <http://doi.org/10.1088/0957-4484/18/32/325103>
- Pollok, B. A., & Heim, R. (1999). Using GFP in FRET-based applications. *Trends in Cell Biology*, 9(2), 57–60. [http://doi.org/10.1016/S0962-8924\(98\)01434-2](http://doi.org/10.1016/S0962-8924(98)01434-2)
- Prindle, A., Liu, J., Asally, M., Ly, S., Garcia-Ojalvo, J., & Suel, G. M. (2015). Ion channels enable electrical communication in bacterial communities. *Nature*, 527(7576), 59–63. Retrieved from <http://dx.doi.org/10.1038/nature15709>
- Psakis, G., Polaczek, J., & Essen, L. O. (2009). AcrB et al.: Obstinate contaminants in a picogram scale. One more bottleneck in the membrane protein structure pipeline. *Journal of Structural Biology*, 166(1), 107–111. <http://doi.org/10.1016/j.jsb.2008.12.007>
- Ren, D., Navarro, B., Xu, H., Yue, L., Shi, Q., & Clapham, D. E. (2001). A prokaryotic voltage-gated sodium channel. *Science (New York, N.Y.)*, 294(5550), 2372–2375. <http://doi.org/10.1126/science.1065635>
- Rigaud, J.-L., & Lévy, D. (2003). Reconstitution of membrane proteins into liposomes. *Methods in Enzymology*, 372, 65–86. [http://doi.org/10.1016/S0076-6879\(03\)72004-7](http://doi.org/10.1016/S0076-6879(03)72004-7)
- Rigaud, J.-L., Levy, D., Mosser, G., & Lambert, O. (1998). Detergent removal by non-polar polystyrene beads. *European Biophysics Journal*, 27(4), 305–319. <http://doi.org/10.1007/s002490050138>
- Riquelme, G., Lopez, E., Garcia-Segura, L. M., Ferragut, J. A., & Gonzalez-Ros, J. M. (1990). Giant liposomes: a model system in which to obtain patch-clamp recordings of ionic channels. *Biochemistry*, 29(51), 11215–11222. <http://doi.org/10.1021/bi00503a009>
- Rottiers, T., Ghyselbrecht, K., Meesschaert, B., Van der Bruggen, B., & Pinoy, L. (2014). Influence of the type of anion membrane on solvent flux and back diffusion in electro dialysis of concentrated NaCl solutions. *Chemical Engineering Science*, 113, 95–100. <http://doi.org/http://dx.doi.org/10.1016/j.ces.2014.04.008>
- Saha, S. C., Henderson, A. J., Powl, A. M., Wallace, B. A., de Planque, M. R. R., & Morgan, H. (2015). Characterization of the Prokaryotic Sodium Channel Na_vSp Pore with a Microfluidic Bilayer Platform. *PLoS ONE*, 10(7), e0131286. Retrieved from <http://dx.doi.org/10.1371/journal.pone.0131286>
- Schild, L., Ravindran, A., & Moczydlowski, E. (1991). Zn²⁺-induced subconductance events in cardiac Na⁺ channels prolonged by batrachotoxin. *Current-voltage*

- behavior and single-channel kinetics. *The Journal of General Physiology* , 97 (1) , 117–142. <http://doi.org/10.1085/jgp.97.1.117>
- Sigg, D., & Bezanilla, F. (1997). Total Charge Movement per Channel : The Relation between Gating Charge Displacement and the Voltage Sensitivity of Activation. *The Journal of General Physiology*, 109(1), 27–39. Retrieved from <http://www.ncbi.nlm.nih.gov/pmc/articles/PMC2217050/>
- Studer, A., Demarche, S., Langenegger, D., & Tiefenauer, L. (2011). Integration and recording of a reconstituted voltage-gated sodium channel in planar lipid bilayers. *Biosensors & Bioelectronics*, 26(5), 1924–8. <http://doi.org/10.1016/j.bios.2010.06.008>
- Sumino, A., Sumikama, T., Iwamoto, M., Dewa, T., & Oiki, S. (2013). The Open Gate Structure of the Membrane-Embedded KcsA Potassium Channel Viewed From the Cytoplasmic Side. *Scientific Reports*, 3, 1063. <http://doi.org/10.1038/srep01063>
- Szoka, F. J., & Papahadjopoulos, D. (1980). Comparative properties and methods of preparation of lipid vesicles (liposomes). *Annual Review of Biophysics and Bioengineering*, 9, 467–508. <http://doi.org/10.1146/annurev.bb.09.060180.002343>
- Tien, H. T., Carbone, S., & Dawidowicz, E. A. (1966). Formation of “black” lipid membranes by oxidation products of cholesterol. *Nature*, 212(5063), 718–719. <http://doi.org/10.1038/212718a0>
- Wiseman, B., Kilburg, A., Chaptal, V., Reyes-Mejia, G. C., Sarwan, J., Falson, P., & Jault, J.-M. (2014). Stubborn Contaminants: Influence of Detergents on the Purity of the Multidrug ABC Transporter BmrA. *PLoS ONE*, 9(12), e114864. Retrieved from <http://dx.doi.org/10.1371/journal.pone.0114864>
- Xu, J., Wang, X., Ensign, B., Li, M., Wu, L., Guia, A., & Xu, J. (2001). Ion-channel assay technologies: Quo vadis? *Drug Discovery Today*, 6(24), 1278–1287. [http://doi.org/10.1016/S1359-6446\(01\)02095-5](http://doi.org/10.1016/S1359-6446(01)02095-5)
- Zakharian, E. (2013). Recording of Ion Channel Activity in Planar Lipid Bilayer Experiments. *Methods in Molecular Biology (Clifton, N.J.)*, 998, 109–118. http://doi.org/10.1007/978-1-62703-351-0_8
- Zhang, X., Ren, W., DeCaen, P., Yan, C., Tao, X., Tang, L., ... Yan, N. (2012). Crystal structure of an orthologue of the NaChBac voltage-gated sodium channel. *Nature*, 486(7401), 130–134. Retrieved from <http://dx.doi.org/10.1038/nature11054>
- Zimmerberg, J., Cohen, F. S., & Finkelstein, A. (1980). Micromolar Ca²⁺ stimulates fusion of lipid vesicles with planar bilayers containing a calcium-binding protein. *Science*, 210(4472), 906–908.